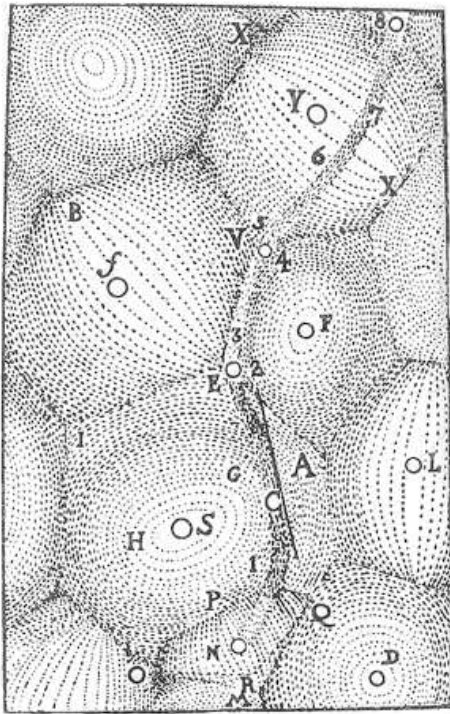


Filaments, Voids, and Pancakes



R. Descartes (1644)

Principia Philosophiae, Pr III 53

Written while Descartes was living in Egmond aan den Hoef in North Holland and prior to his move to Sweden.

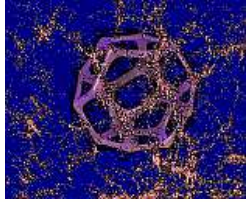
He left France because of intellectual persecution by the Dutch theologian Gisbert Voetius, an anti-Cartesian zealot.

The structural elements of the Cosmic Web

Bernard Jones

*Kapteyn Astronomical Institute,
Groningen, NL*

Presented at
IAU Symposium 308
**The Zeldovich Universe:
Genesis and Growth of the Cosmic Web**
Tallinn, Estonia, June 23-28, 2014



The Groningen Team

Topics covered:

- ❑ Zel'dovich legacy
- ❑ Finding structure: the tools
 - Segmentation and Simulation
 - Visualisation and Analysis
- ❑ Visualisations: a few examples
 - MMF/NEXUS and others
 - Adhesion and phase space
- ❑ Mechanics of structure finding
 - DTFE resampling
 - Multi-scale Hessian Analysis
 - Finding Voids: Watershed
- ❑ Dynamical evolution
 - Dynamical drivers
 - Spin + Angular Momentum
- ❑ What next?

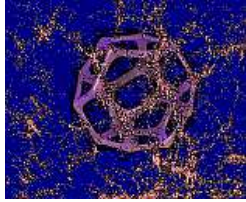
Rien van de Weygaert
Bernard Jones

The team:

- ❑ Patrick Bos
- ❑ Matthijs Dries
- ❑ Job Feldbrugge
- ❑ Johan Hidding
- ❑ Pratyush Pranav
- ❑ Stephen Rieder

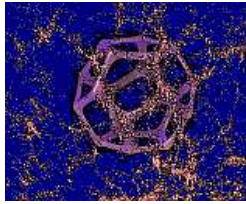
and in collaboration with

- ❑ Carlos Frenk
- ❑ Marius Cautun



Where this all started

- ❑ In 1970 Zel'dovich published a nonlinear model for the evolution of initially small amplitude fluctuations which implied a universe with structure dominated by voids, their surrounding walls (“pancakes”). Intersections of walls would be filaments and clusters.
- ❑ As the decades went by, redshift catalogues of ever more distant galaxies revealed this structure.



Zel'dovich's Legacy (1970)

A kinematic (ballistic) approximation, no pressure, no viscosity

At time t , a particle initially at \mathbf{q} is at \mathbf{x} , given by

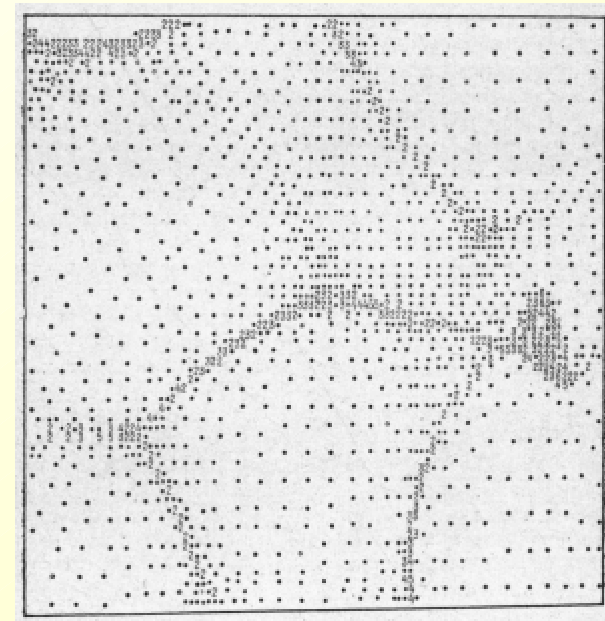
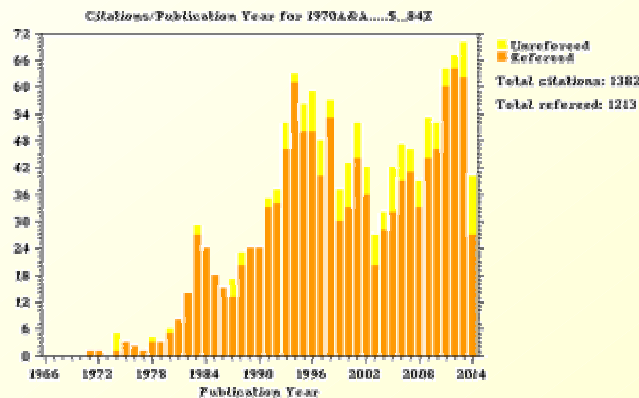
$$\mathbf{x} = \mathbf{q} - D(t)\boldsymbol{\psi}(\mathbf{q})$$

$D(t)$ is the growth rate factor

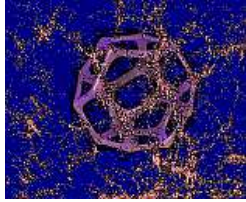
$\boldsymbol{\psi}(\mathbf{q})$ is the Zel'dovich deformation tensor

If $\boldsymbol{\psi}(\mathbf{q})$ has eigenvalues $\gamma_1 \geq \gamma_2 \geq \gamma_3$ then

$$\frac{\rho(\mathbf{x}, t)}{\rho_0(t)} = \left\| \frac{\partial \mathbf{x}}{\partial \mathbf{q}} \right\|^{-1} = \frac{1}{[1 - D(t)\gamma_1][1 - D(t)\gamma_2][1 - D(t)\gamma_3]}$$

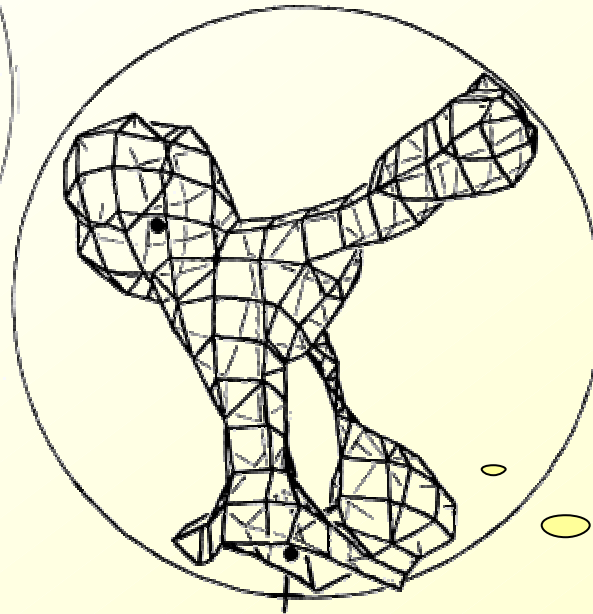
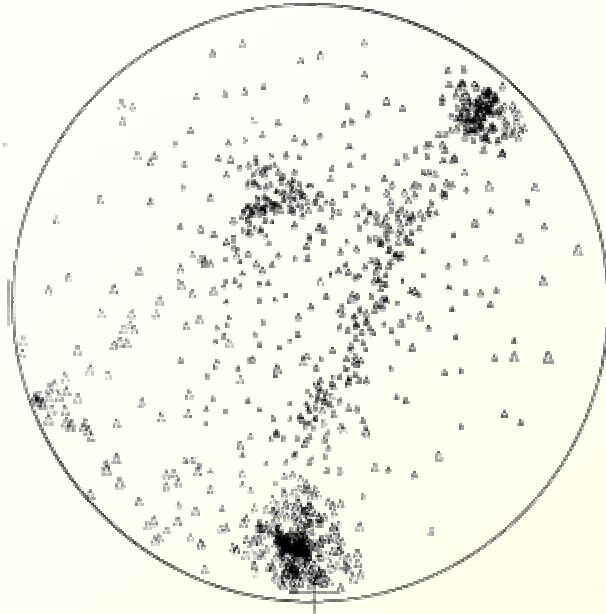


The first 2-D view of the prediction of the Zel'dovich model for the nonlinear evolution of cosmic structure. **Shandarin (1976)**



Klypin-Shandarin Simulation

Three-dimensional numerical model of the formation of large scale structure in the universe.
Monthly Notices, **1983**, **204**, 891

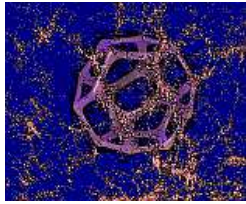


From the abstract:

“The structure formation begins from pancakes, then evolves to the network structure, then to the formation of clumps connected by strings and afterwards to the formation of huge isolated clumps.”

- ❑ 32^3 particles
- ❑ Initial conditions using Zel'dovich approximation
- ❑ PM evolution code

Is this
a headless
chicken?



Early redshift survey maps

From the Z-cat paper:

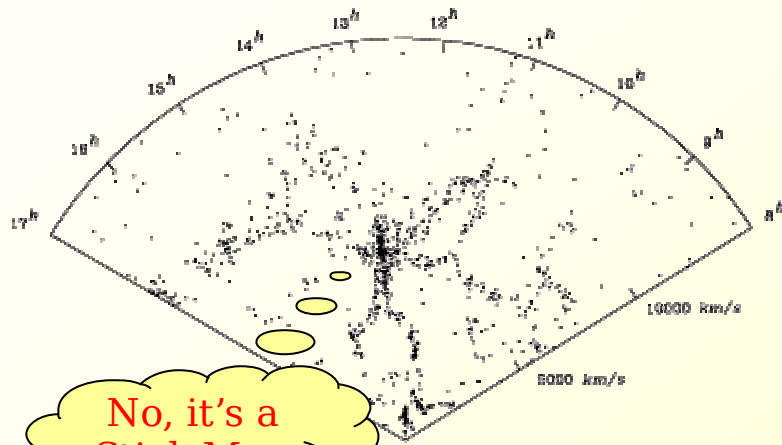
The intermediate and distant redshift windows ... exhibit clustering in frothy, almost filamentary, patterns of connectedness surrounding empty holes on the sky.

M. Davis, J. Huchra, D.W. Latham, J. Tonry.

"A survey of galaxy redshifts.

II - The large scale space distribution"

Astrophysical Journal, Part 1, vol. 253, **1982**, p. 423-445



No, it's a Stick Man

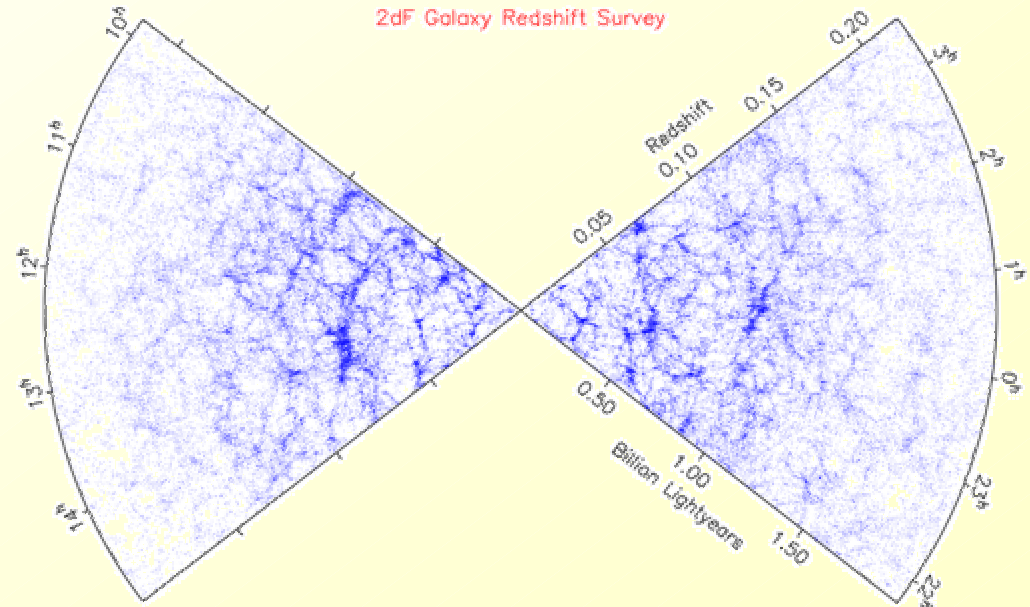
V. de Lapparent, M.J. Geller and J.P. Huchra.

"A slice of the Universe"

Astrophysical Journal Letters **1986**, vol 302, L1-L5.

The great 2dF survey marked a transition in the running of surveys, analysis techniques and the dissemination of the data

2dF Galaxy Redshift Survey

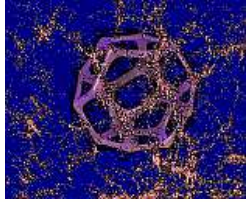


Matthew Colless et al. (the 2dFGRS team), **2003**

"The 2dF Galaxy Redshift Survey: Final Data Release"

From <http://arxiv.org/abs/astro-ph/0306581>

Survey website: <http://magnum.anu.edu.au/~TDFgg/>

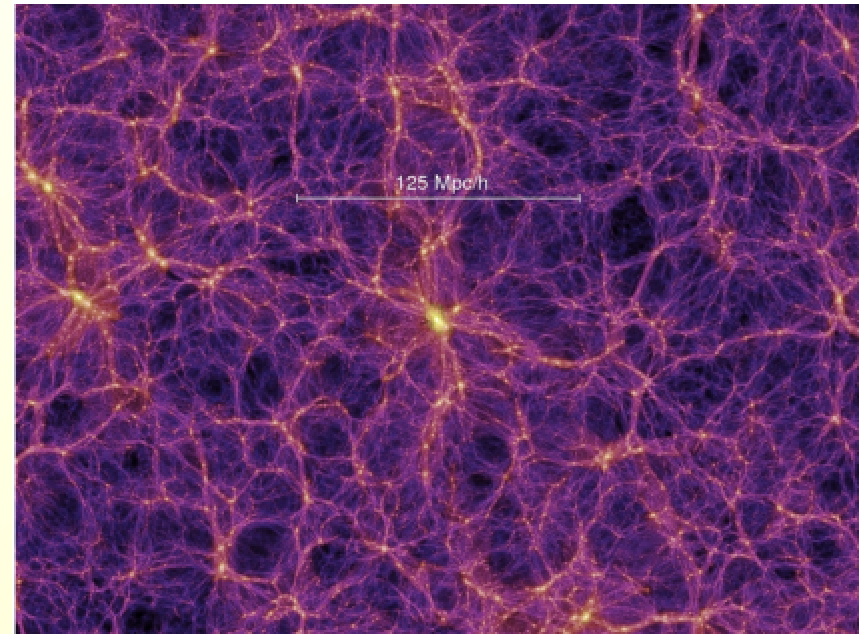
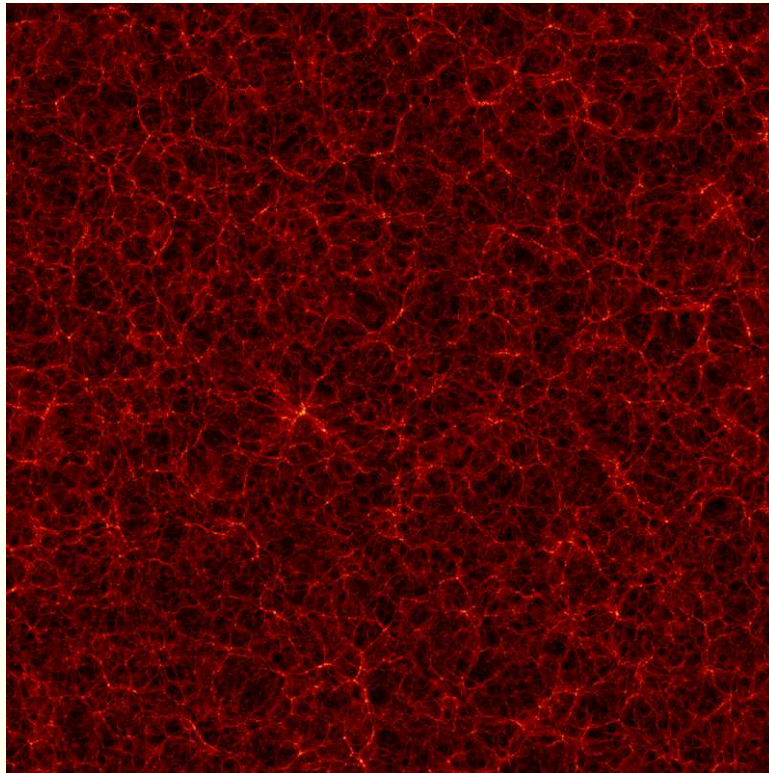


Structure in N-body simulations

Filaments of dark matter dominate the visual appearance of simulations.

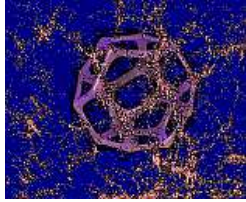
Below:

Bolshoi MultiDark Simulation. Slice at $z = 0$.
The simulation box is 1000 Mpc/h on a side and
the slice is again 5 Mpc/h thick. (Stefan Gottlöber)
Klypin et al. 2011, Astrophysical Journal



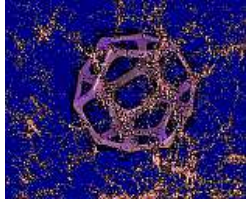
Above:

Millenium Simulation, slice at $z=0$.
Luminous matter, based on semi-analytic models for
star formation, has been added. This is only a part
of the main simulation box.
(Springel et al. 2005, Nature)



Finding structure: the tools

- ❑ We perceive structure in observational data and in computer simulations (N-Body models). We need methods to systematically and consistently identify that structure.
- ❑ This aids in both the visualisation of that structure and in quantifying the dynamical processes that form the environments for galaxy formation.



Visualisation, Segmentation, Simulation and Analysis

❑ Visualisation

- Optimising data for the purposes of presentation
- Involves “cleaning” and “rendering”
- Uses transformations of the data space
Can transform both the coordinates and the data

❑ Segmentation

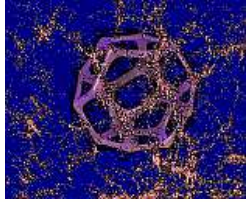
- Discovering and identifying the “content” of a data set
- Finding the perceptually distinct components
- These may or may not be dynamically significant
- Enhanced by transformations of the data space

❑ Simulation

- Static simulation is a mathematical model for the data
- Dynamic simulation is how the data came to be and may involve a variety of approximating models

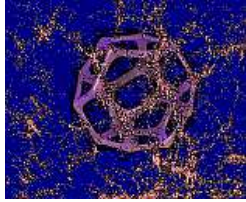
❑ Analysis and understanding

- Image Processing
- Depends on, and is a part, of all of the above



Why segmentation is important

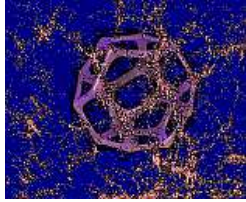
- ❑ Goal is to identify structural environments
 - Voids, Walls, Filaments, Clusters
 - Make perceptual sense (what we see)
 - Make mathematical sense (eigenvalues)
 - Make dynamical sense (how it got there)
- ❑ Many ways of finding particular structures
 - Void comparison project
 - Cosmic Web comparison project
- ❑ Need consistent procedures, preferably ...
 - **Parameter-free**
 - **Scale independent**
 - Reflect perceptual, mathematical and dynamical aspects of structure
- ❑ Provide targets for observations of galaxies in structurally defined environments
 - Samples selected on basis on geometry



Structure Finding Methodologies

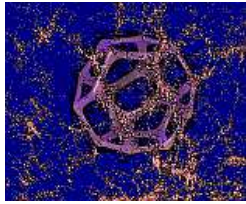
Paper of Forero-Romero, Contreras and Padilla **2014** arXiv 1406.0508
“Cosmic web alignments with the shape, angular momentum and peculiar velocities of dark matter halos” has nice overview.

- ❑ Dynamical (needs velocity or potential information)
 - ORIGAMI (Falck, Neyrinck)
 - KHA (Khaeler, Hahn, Abel)
 - T-web and V-web (Libeskind, Forero-Romero, et al.)
 - Hessian of gravitational Potential (Hahn, Porciani, Dekel, et al.)
- ❑ Geometric / Topological
 - MMF/NEXUS (Aragon-Calvo, Cautun, van de Weygaert, Jones, et al.)
 - SHMAFF (N. Bond, Strauss, Cen)
 - MAK (Lavaux, Wandelt, Sutter, Mohayee et al.)
 - WVF/ ZOBOV (Platen, van de Weygaert, Jones, Neyrinck, et al.)
 - Morse (Codis et al.)
 - Skeleton (Sousbie, Colombi, Pichon, Pogosyan, et al.)
 - Spineweb (Aragon-Calvo, van de Weygaert, Platen, et al.)
- ❑ Point-set
 - Candy (Stoica, Martinez, Saar)
 - Bisous (Stoica, Temple, et al.)



Visualisations: a few examples

- ❑ We need to visualise data defined on either on a grid, or at a set of discrete points. In the latter case we have to resample the data on grid.
- ❑ When we look at a “data cube” there is often no supplementary data that helps improve on simple image rendering. So we make the most of what we have.
- ❑ Sometimes, as when we have information about the entire phase space, we may be able to use the additional information to enhance the view of the data cube.



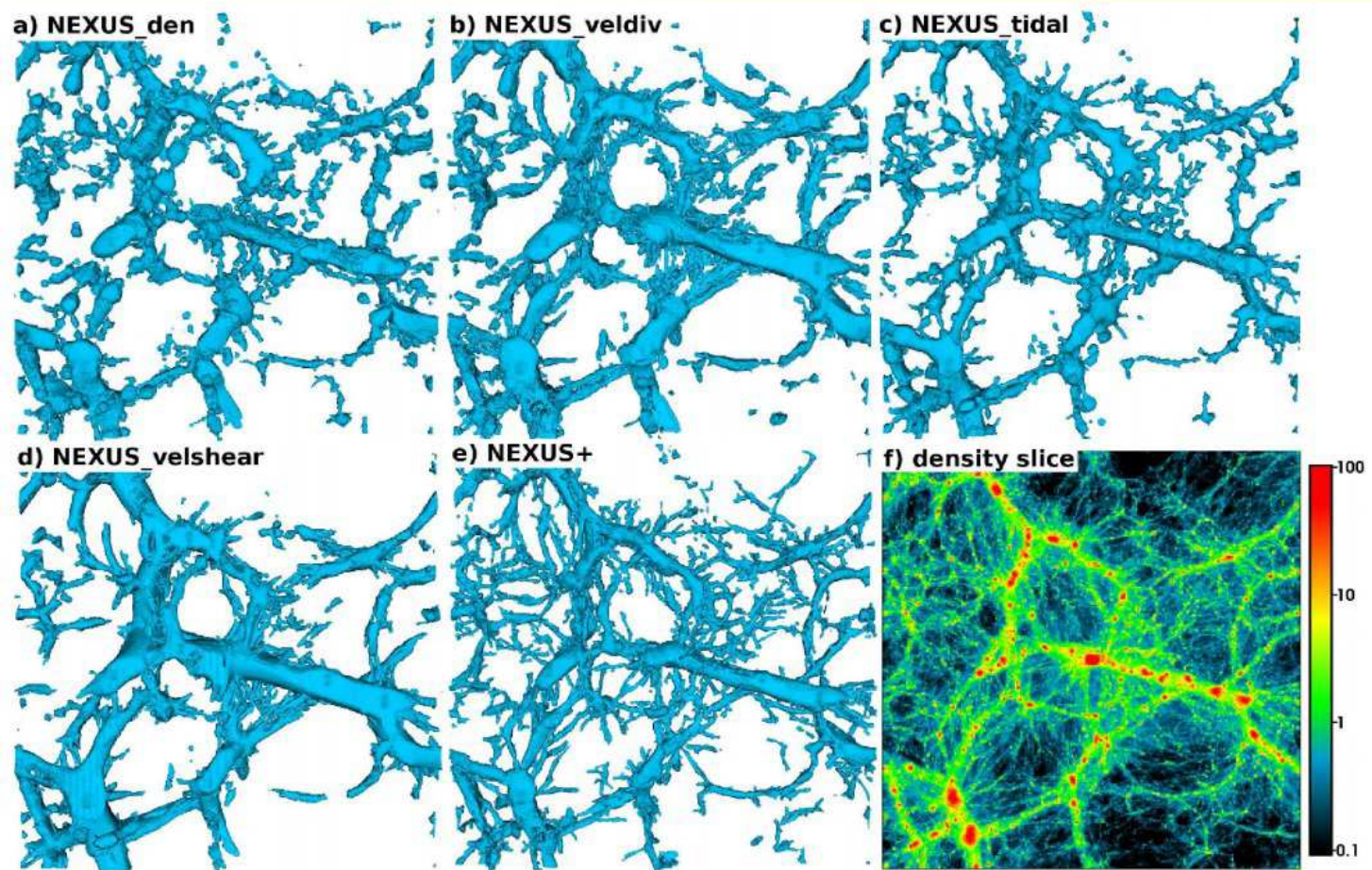
NEXUS: different fields

NEXUS can evaluate structures using different functions defined on the point set.

This, not surprisingly, produces different maps of the cosmic web structures.

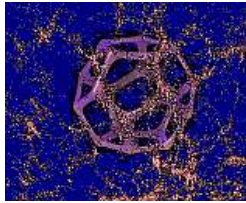
The relationship between these maps reflects the influence of the underlying physics.

NEXUS+ uses the log-density field to determine structure and is particularly effective in low density areas.



NEXUS is part of a long-term project of Rien van de Weygaert to analyse the physics of the cosmic web. It is developed as part of the PhD Thesis of Marius Cautun (University of Groningen, 2013).

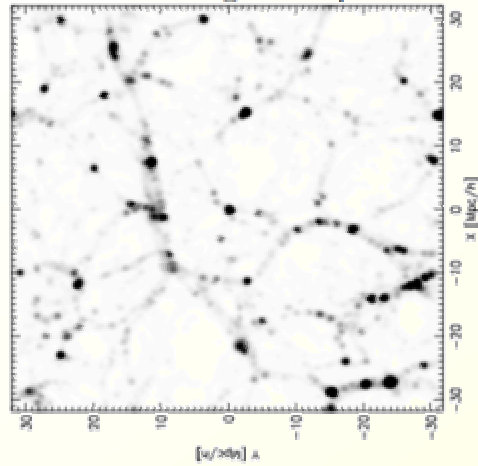
*Cautun et al. <http://arxiv.org/abs/1209.2043>, (MNRAS **129**, 1286, 2013),*



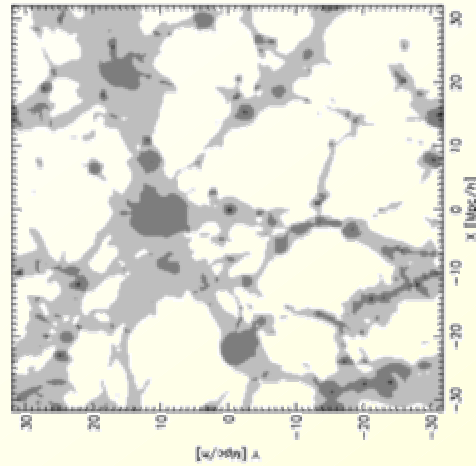
Structure in CLUES

Image from a talk by Noam Libeskind

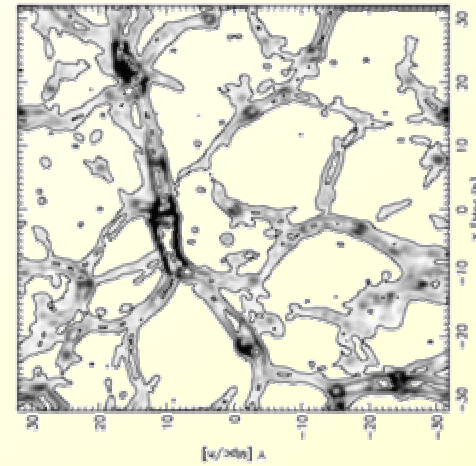
Log density



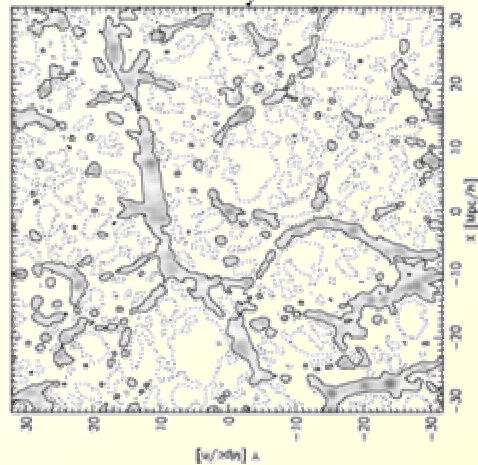
Tidal Tensor



div . v



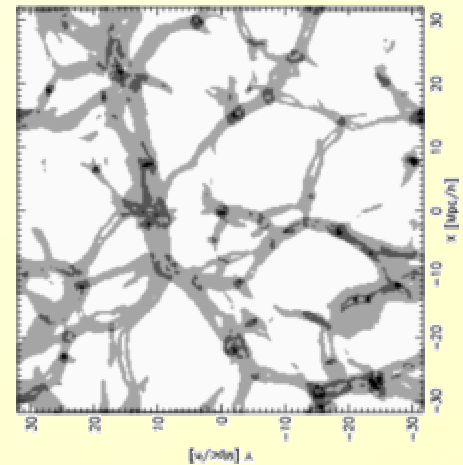
density

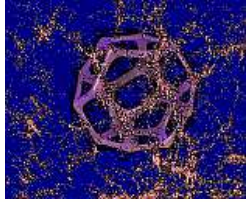


Use a 2048^3 DM only simulation
64 Mpc box –

512^3 grid, $R_{\text{smooth}} = 0.125 \text{ Mpc}/h$

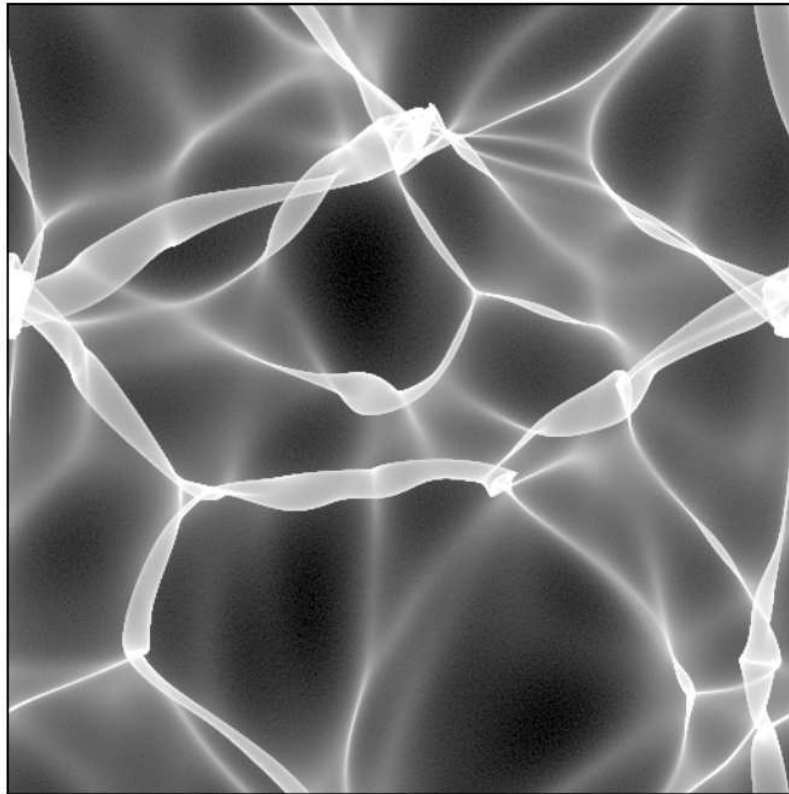
Shear



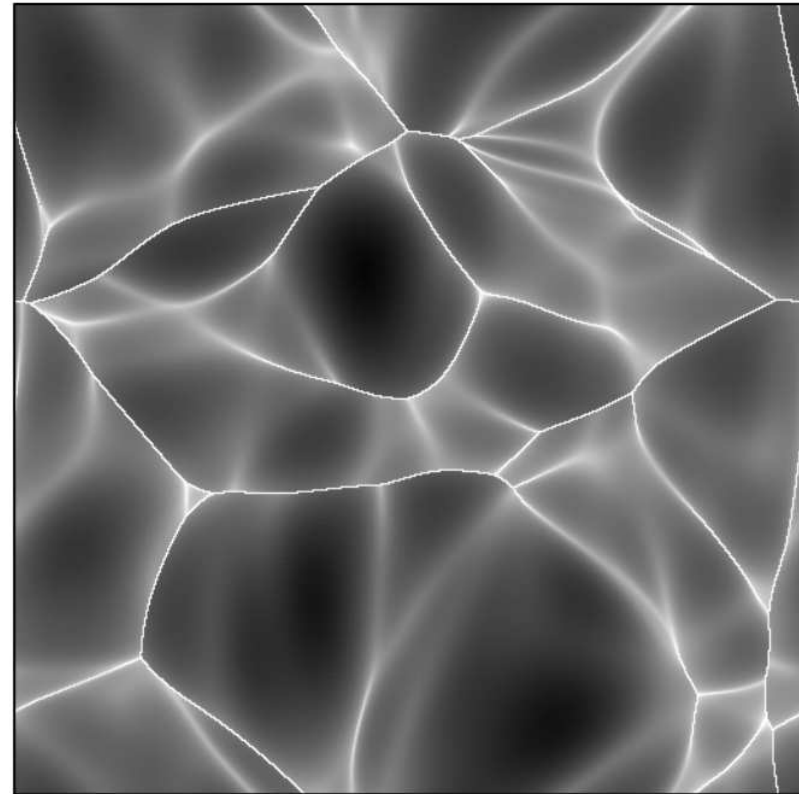


Adhesion: modified Zel'dovich

Zeldovich

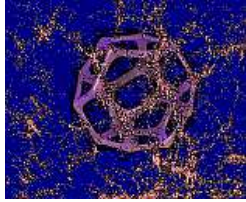


Adhesion



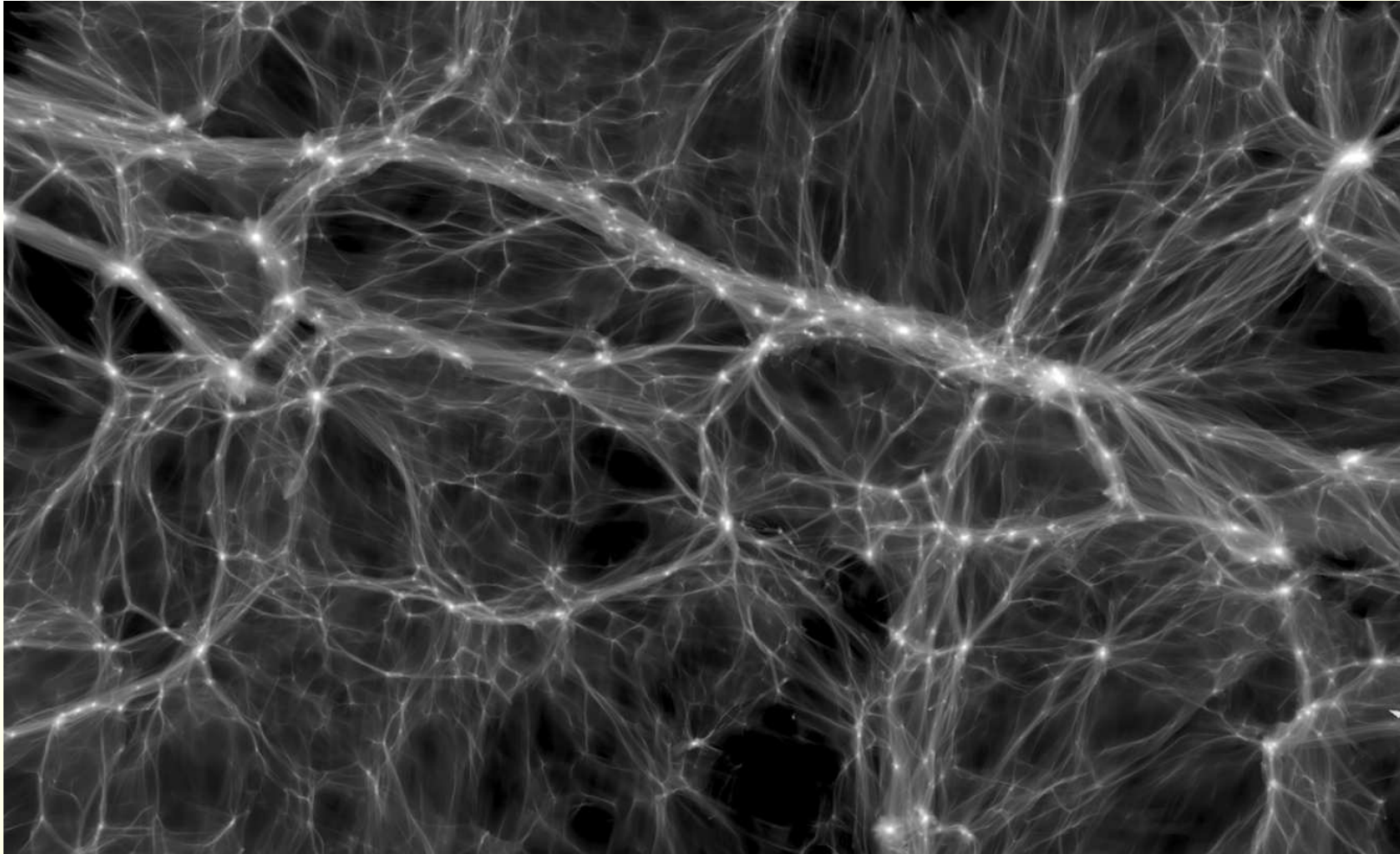
Pictures courtesy of Johan Hidding

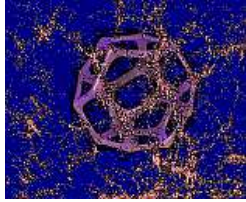
Comparison of Zel'dovich approximation and adhesion. The models were evolved in two dimensions according to the Zel'dovich approximation and adhesion. Multi-streaming has occurred in the Zel'dovich model. The viscosity in the adhesion model prevents multi-streaming and filaments are formed. The models only differ where multi-streaming has occurred.



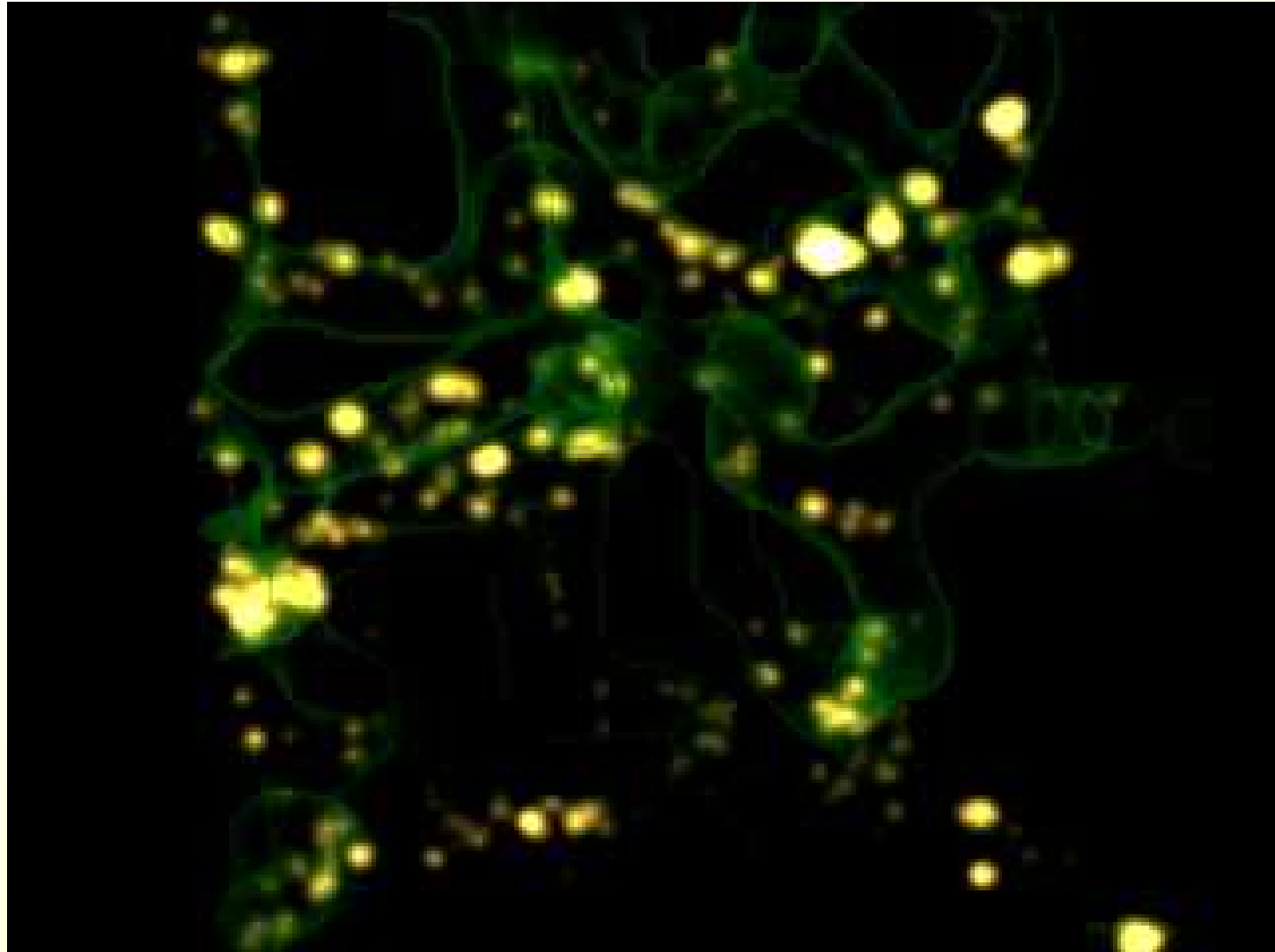
Phase-space reconstruction

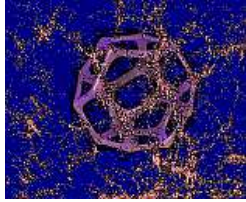
From T. Abel, O.Hahn and R. Kaehler, 2012 M.N.R.A.S. 2012, 427, 71-76.
"Tracing the Dark Matter Sheet in Phase-Space"





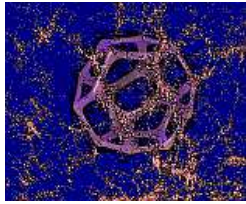
Filaments in DR6 (Aragon-Calvo)





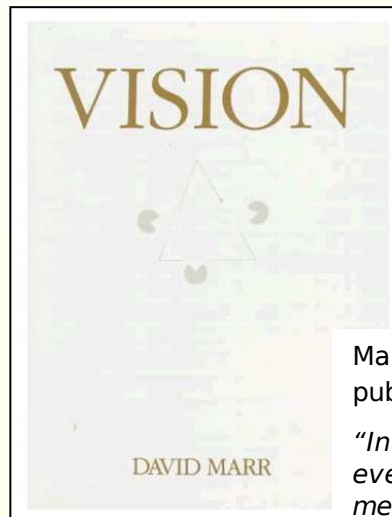
Mechanics of structure finding

- ❑ There are now many methods of doing this. This is how we use scale-space to do it and achieve a method that is scale-independent and parameter-free.
- ❑ Like all techniques, the final visualisation needs a method of prettifying (ie:rendering) the data.



Perceptual models for feature recognition

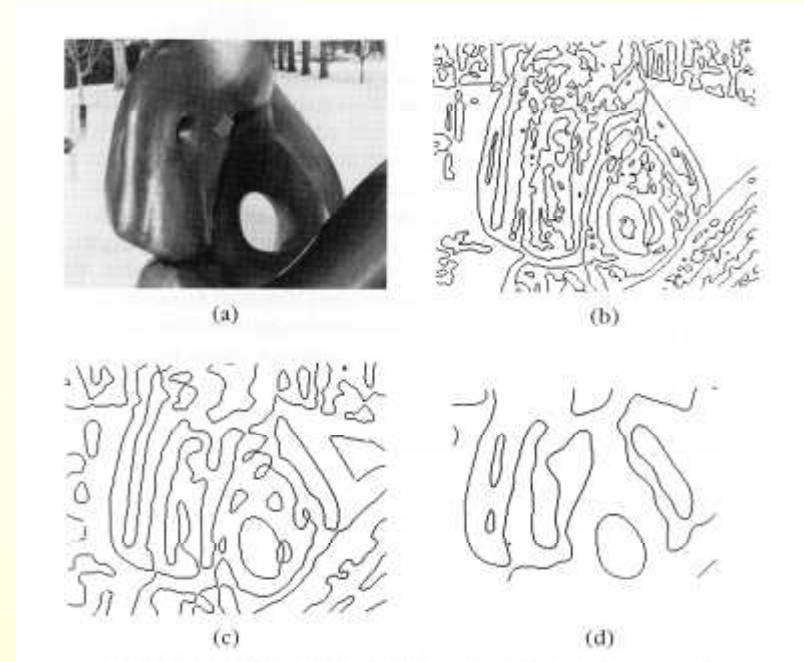
- ❑ Goes back to David Marr's "Primal Sketch" (1976)
Phil. Trans. Roy. Soc. (B), **275**, 483, 1976
- ❑ Generalised during the 1990's for use in radiological diagnosis.
- ❑ Now replaced by other more powerful methods (eg: Canny)



Marr presented the primal sketch as a model for how the eye and brain interpret what is seen.

Marr's seminal work was published posthumously:

"In December 1977, certain events occurred that forced me to write this book a few years earlier than I had planned"

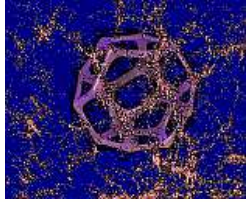


From "Vision" by David Marr (1982)

The picture e_r is smoothed by a sequence of Gaussians. The contours correspond points

where $\mathcal{L}^2 e_r = 0$.

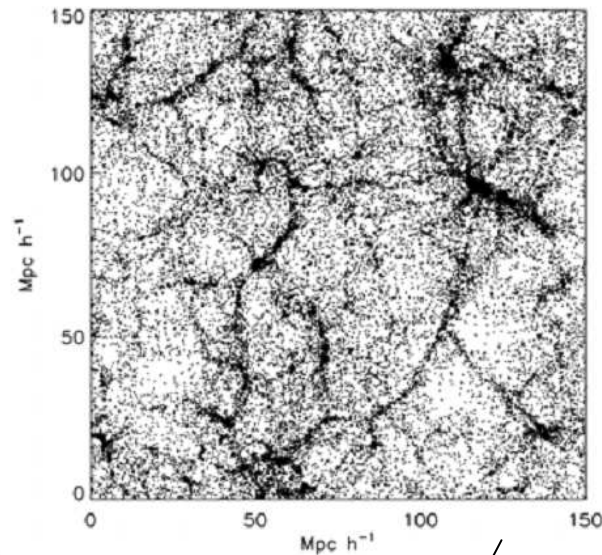
Obviously the smoother pictures show the simpler contours with better delineation of features.



Scaling analysis – MMF et seq.

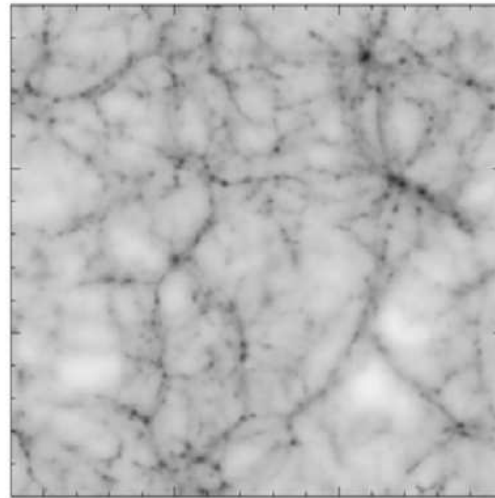
The Multiscale Morphology Filter
Aragon-Calvo, Jones, van de Weygaert, van de Hulst
ApJ Lett, 655, L5 2007, A&A, 474, 315. 2007

Particle distribution



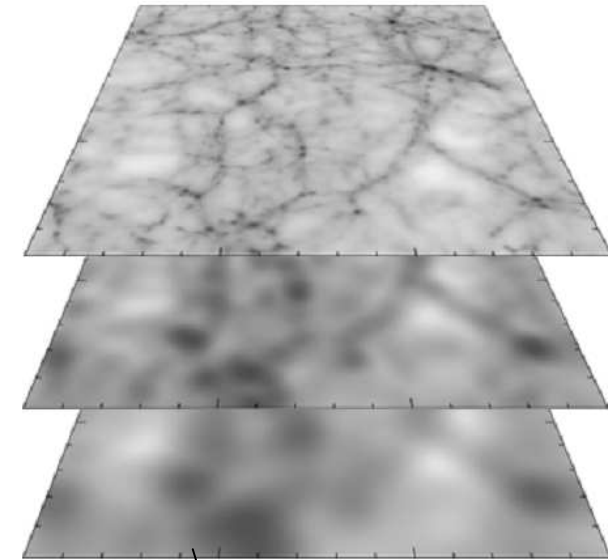
The starting data is a point set from a galaxy catalogue or a simulation

Density field



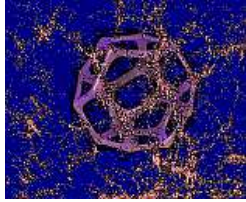
Construct a continuous density map using Delaunay Triangulation

Scale space



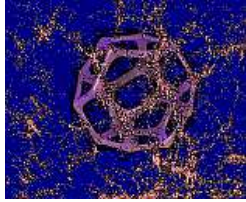
See which features are **persistent** through all scales.
But how do you find these features?

Doing precision cosmology demands an accurate and quantitative assessment of structure.



Hessian-based multiscale methods

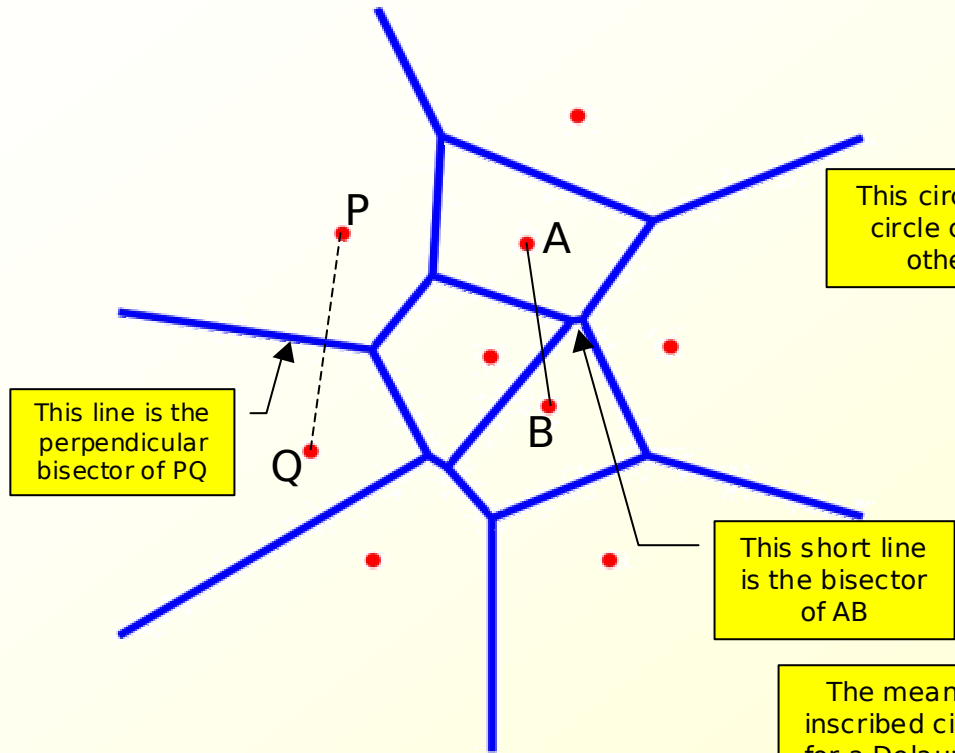
- ❑ There are many web structure analysis techniques, but relatively few are multi-scale.
- ❑ The power of NEXUS+ is that it also probes weak structure in under-dense regions. This is crucial since we find galaxies there.
- ❑ Filaments have 50% of the cosmic mass while occupying only 10% of the volume.
- ❑ Filaments have their own special dynamics which has consequences for galaxy formation.



Voronoi and Delaunay

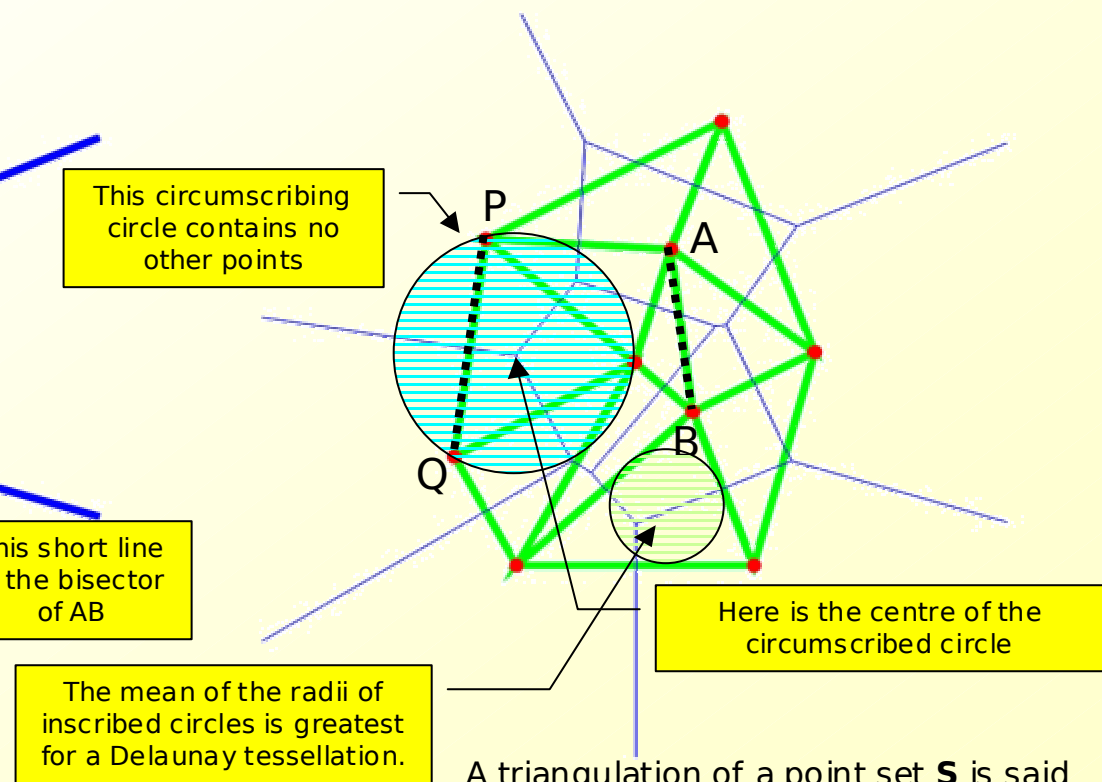
From discrete point sets to continuous fields and topology

Voronoi tessellation

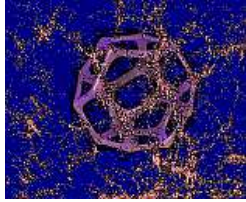


The **Voronoi cell** of a point in a set **S** is the region that is closer to the point than to any other point of the set **S**.

Delaunay triangulation



A triangulation of a point set **S** is said to be **Delaunay** if the interior of the circumcircle of any triangle in the triangulation contains no points of **S**.



DTFE: from points to grid

Delaunay Triangulation Field Estimator

R. van de Weygaert and W. Schaap in "Data Analysis in Cosmology",
Lecture Notes in Physics, Springer 2009, 665. p.291-413

Edited by V. J. Martínez, E. Saar, E. Martínez-González, and M.-J. Pons-Bordería.

M. Cautun and R. van de Weygaert. **The DTFE public software**. 2011.

URL: <http://arxiv.org/pdf/1105.0370v3.pdf>

The DTFE provides an optimal estimate of the values of data defined at irregularly spaced points.

$$\widehat{\rho}(\mathbf{x}_i) = (1 + D) \frac{m_i}{V(\mathcal{W}_i)}$$

D = dimension (2 = plane)

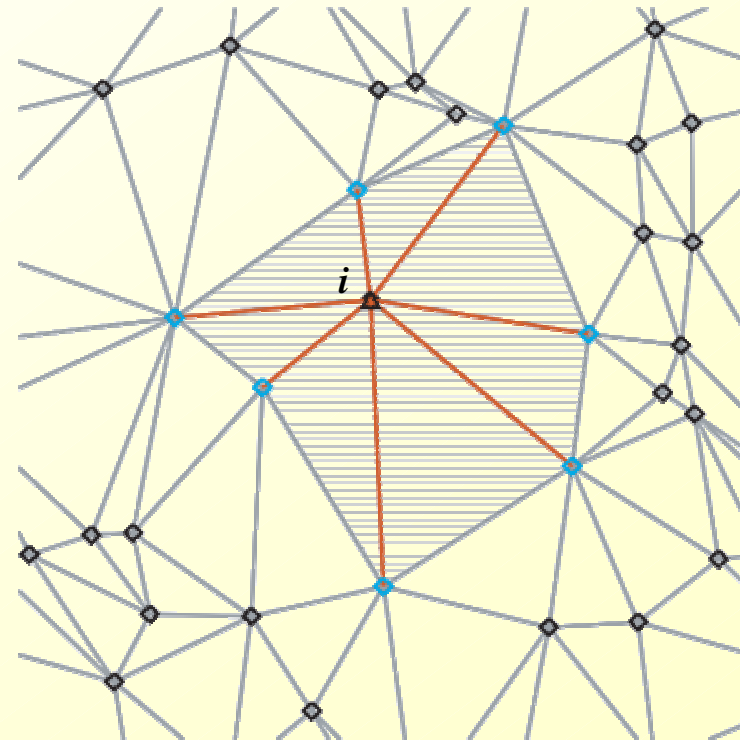
V = volume of Delaunay triangles about the point i .

(see figure on right)

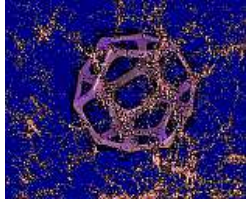
DTFE additionally provides the basis for linear and nonlinear interpolation of data defined on such a point set.

$$\widehat{f}(\mathbf{x}) = \widehat{f}(\mathbf{x}_i) + \nabla \widehat{f}|_m \cdot (\mathbf{x} - \mathbf{x}_i)$$

Linear interpolation within each cell based on simple gradient estimator from points defining the cell.



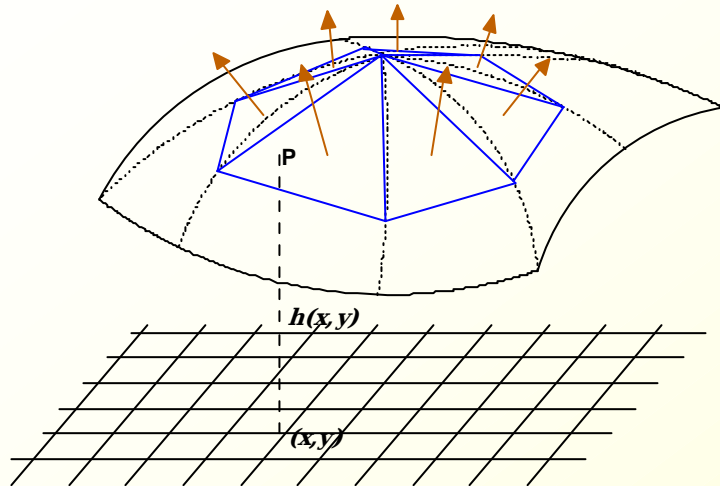
Platen, E., van de Weygaert, R., Jones, B.J.T., Vegter, G. and Aragon-Calvo, M.
"Structural analysis of the SDSS Cosmic Web - I
Non-linear density field reconstructions"
M.N.R.A.S., 2011, 416, 2494-2526 .



Triangulations: surfaces

Calculating local geometric surface properties when surface is specified at discrete points

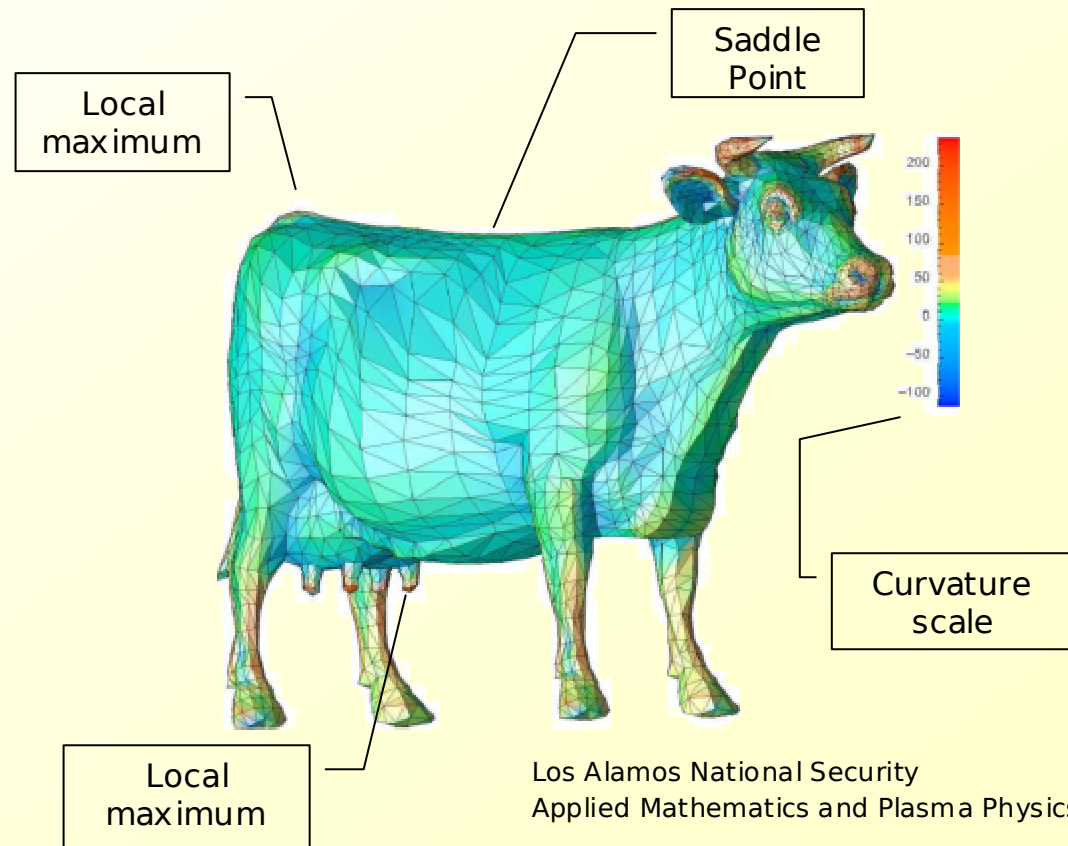
Curvature of surface can be calculated directly from normals to triangles about a point



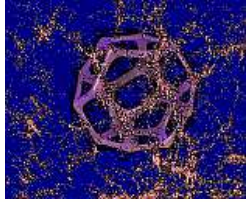
Curvature can be also calculated by interpolating a height function $h(x,y)$ that describes the surface and finding the eigenvalues of the **Hessian**:

$$H_{ij} = \frac{\partial^2 h}{\partial x_i \partial x_j}, \quad i, j = 1, 2$$

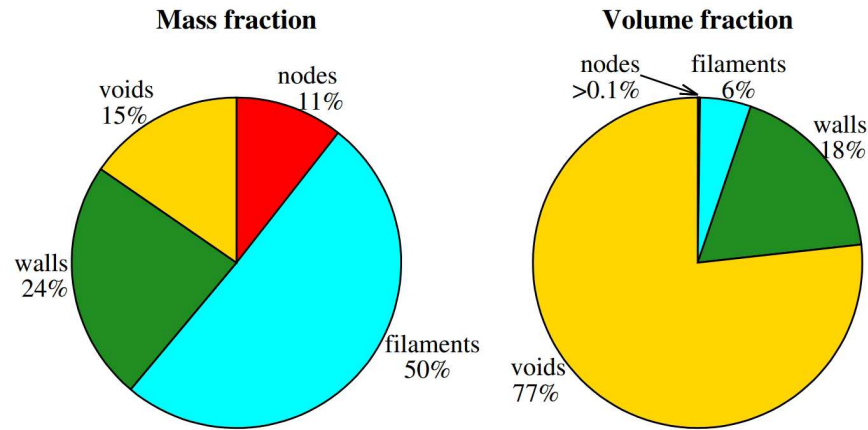
in 2D, with $i, j = 1, 2, 3$ in 3D



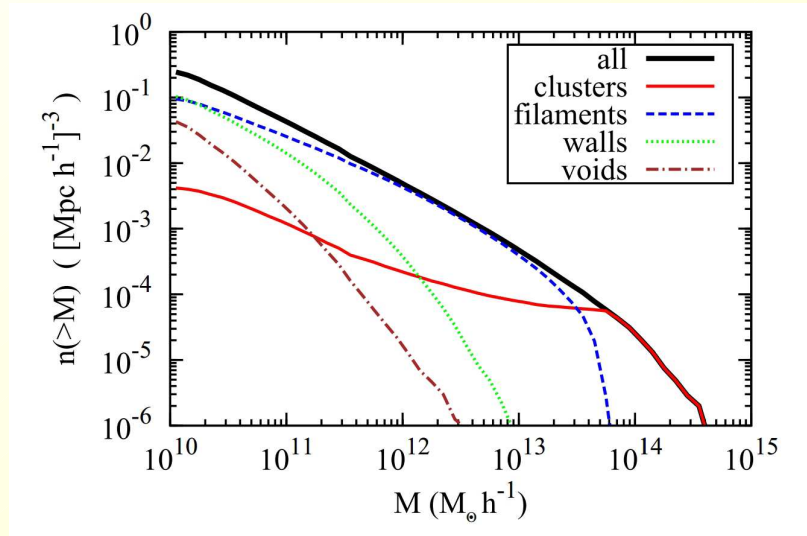
Los Alamos National Security
Applied Mathematics and Plasma Physics



Present day environments

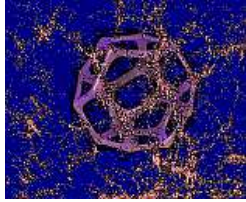


The mass and volume fractions occupied by cosmic web environments detected by the NEXUS+ method.



Present day cumulative halo mass function in cosmic web environments, normalised by volume.

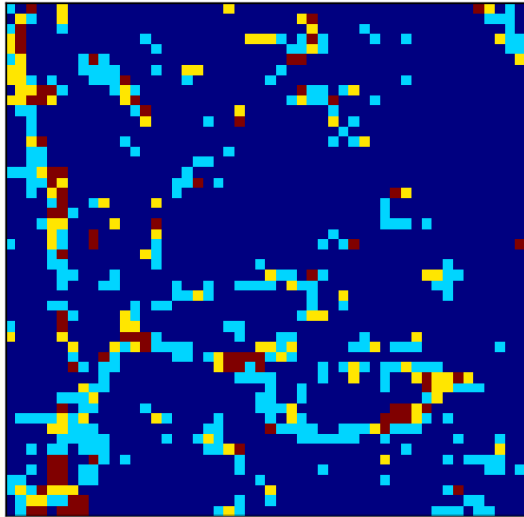
- ❑ Different structure identification methods yield different fractions because of different biases in identification and even in different definitions of each environment.
- ❑ For example, there is a difference in the “nodes” of a factor 3 when using MMF and NEXUS.



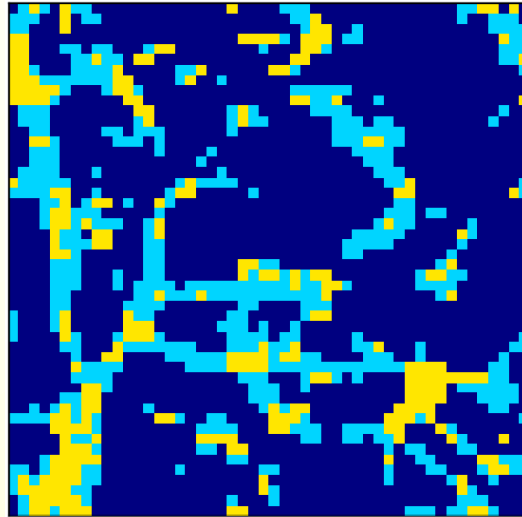
Cosmic Web structure identification

From “*Tracing the Cosmic Web*” workshop held at Lorentz Centre, Leiden
Organised by R. van de Weygaert and N. Libeskind. (17-21 Feb 2014)

Not Rendered – colours indicate nature of feature at each point

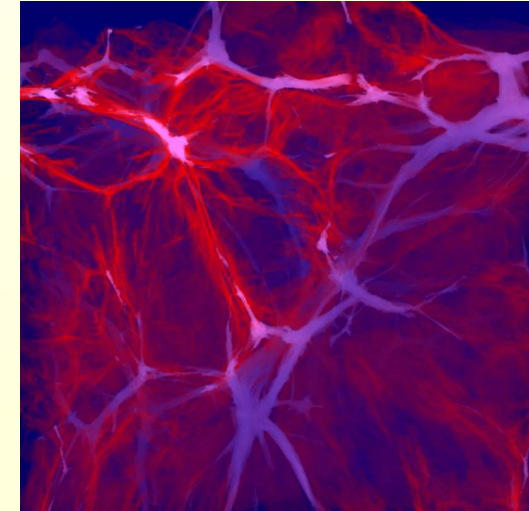


Origami (Neyrinck et al.)
Lagrangian method using
phase space information to
determine structure in
terms of “folding”



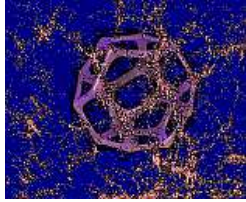
Nexus+ (Cautun et al.)
Uses only position space,
log density information.
Method is parameter free
and multi-scale.

Rendered



Kaehler et al. 2011
Tetrahedral rendering of streaming.
Phase space (6-D) method.
Colours denote number of streams
and hence classification of structure
at each point

The level of agreement between the 3-D and 6-D methods
is encouraging: it means that what we see in 3-D is
dynamical relevant. *But why should this be?*



Voids – much ado about nothing

Shakespeare, 1598

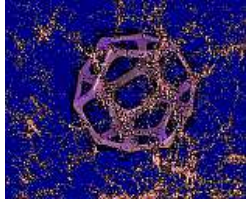
Sheth and van de Weygaert, 2004

- ❑ Voids are distinctly recognisable objects
- ❑ They contain little luminous matter
- ❑ They are not empty: they are full of small scale structure often associated with void galaxies
- ❑ There is a void hierarchy discussed in detail by Sheth and van de Weygaert (2004)
- ❑ We now have methods to reveal that hierarchy in the finest detail

Matthijs Dries (Masters Thesis, Univ. Groningen)

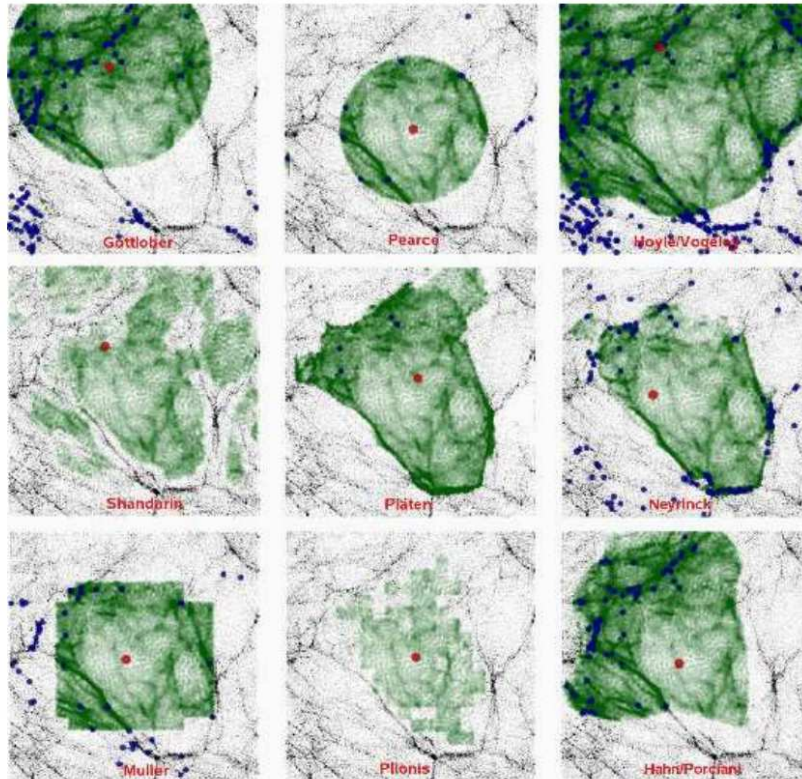
Dries and van de Weygaert (2014), in preparation

See also subsequent slides on NEXUS and Cautun et al, (2013)



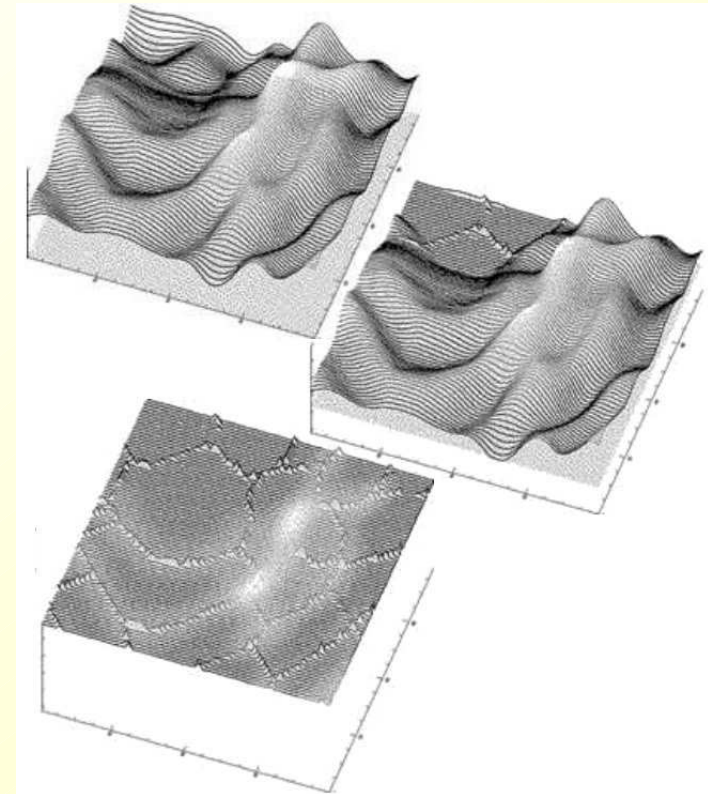
Watershed Void Finder

WVF: E. Platen, R. van de Weygaert, B. Jones, 2007, M.N.R.A.S., **380**, 551
ZOBOV: M.C. Neyrinck, 2008, M.N.R.A.S., **386**, 2101.

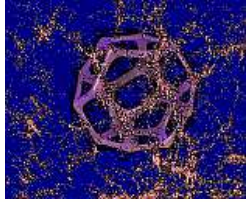


From Colberg et al. MNRAS, 360:216, 2005
 Erwin Platen (Ph.D. thesis, Kapteyn)

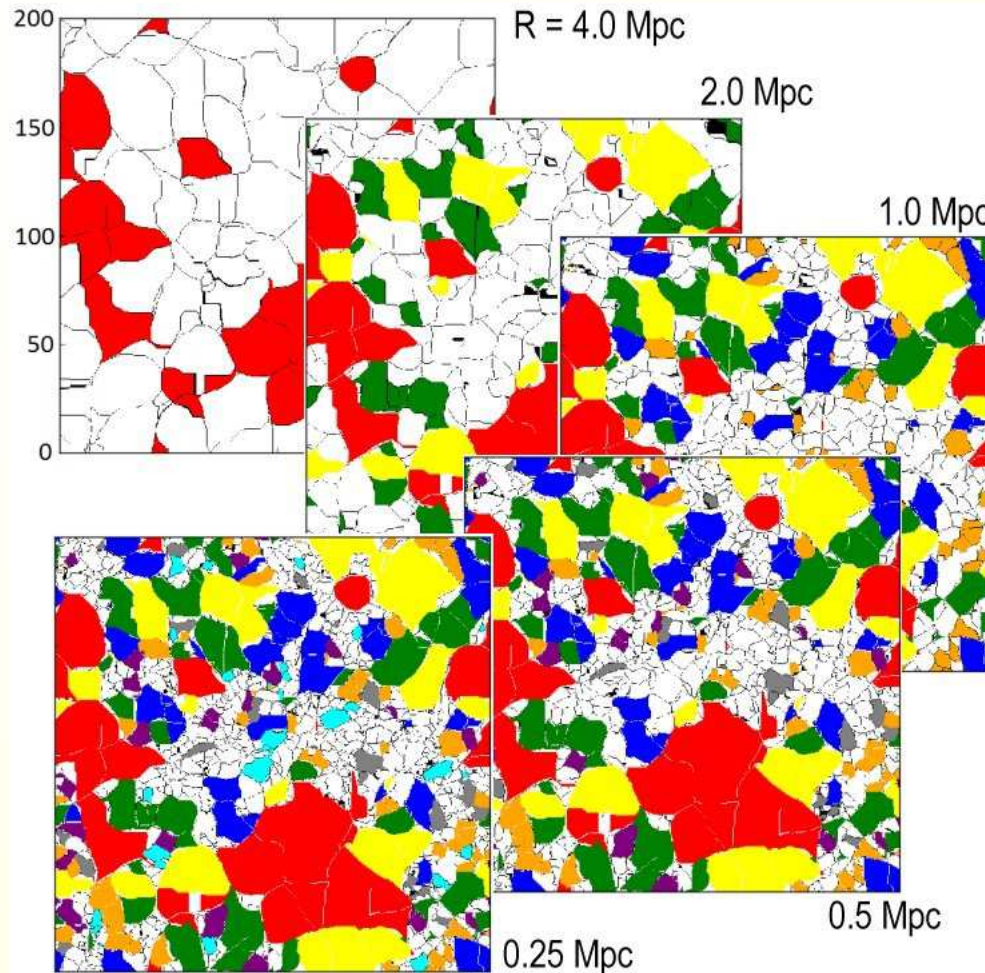
Note that void finders are not filament finders



The metaphor is that, as the water level rises, the valleys get filled and merge when overflow occurs (through saddle points).



Multiscale void finder

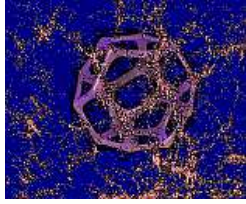


Need to correct some of the downsides of WVF, eg. not all watershed basins necessarily correspond to real voids

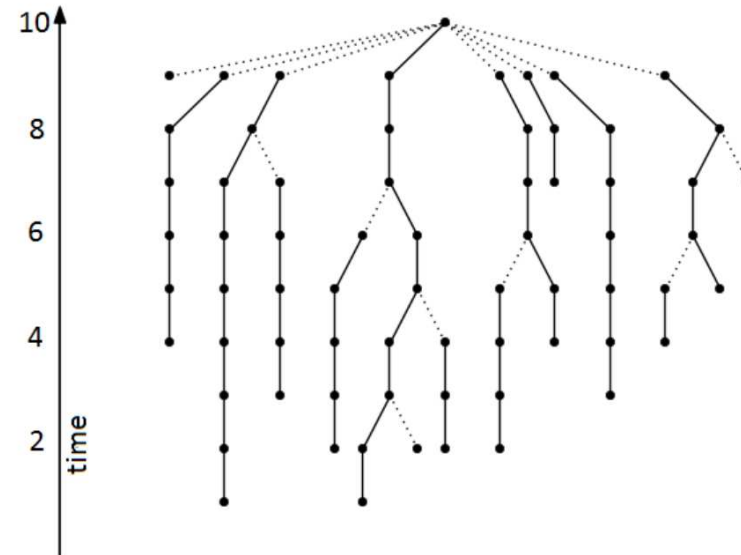
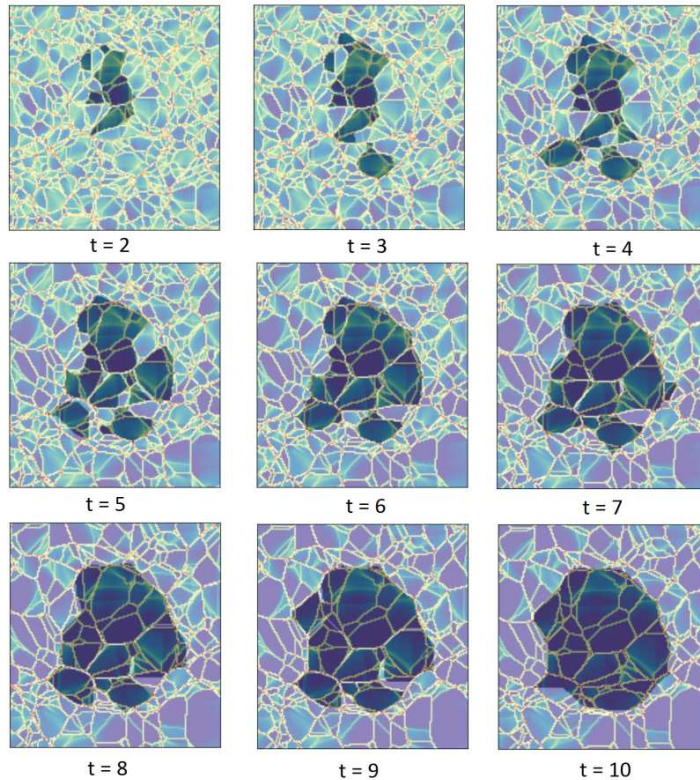
- ❑ The 'emptiness', \mathcal{M}_c , of a watershed basin is the percentage of its grid points that have a density below $\frac{\rho}{\rho_{sc}}$.
- ❑ Require $\mathcal{M}_c > \mathcal{M}_{c,thr}$ for "real" void
- ❑ Big voids will absorb or annexe a smaller void if a 20% fraction of its volume encroaches into the big void.

Colours of the voids correspond to voids detected for a filter radius of
 4 Mpc (red), 3 Mpc (yellow), 2 Mpc (green),
 1.5 Mpc (blue), 1 Mpc (orange), 0.75 Mpc (purple),
 0.50 Mpc (grey) and 0.25 Mpc (cyan).

From the M.Sc. Thesis of Matthijs Dries. Work in progress

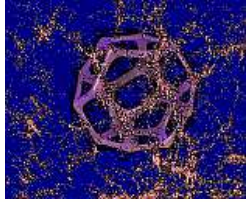


Void merger hierarchy (2-D)



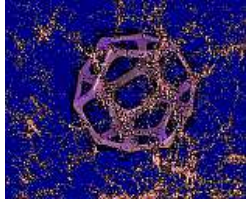
From Matthijs Dries' Master Thesis
(University of Groningen, 2013)

This void hierarchy simulation was made for the purposes of illustration with a 2-dimensional adhesion model having a $P(k) \propto k^{-n}$ power spectrum.



Dynamical evolution

- ❑ Making pretty pictures is all well and good, but structure mapping must be related to the putative underlying dynamical processes.



Drivers of Structure

These quantities are not independent.
In a **compressible fluid** they are linked by the Navier Stokes Equations, which in terms of time derivatives following the fluid motion are:

$$\frac{d\mathbf{V}}{dt} + \mathbf{V}^2 = -\mathbf{P} + \nu \nabla^2 \mathbf{V}, \quad \{\mathbf{V}\}_{ij} = \frac{\partial v_i}{\partial x_j}$$

\mathbf{P} contains Hessians of the gas pressure and the gravitational potential, and will depend on density (eliminated via an equation of state).

ν is a kinematic viscosity of some sort.

This equation can be rewritten as two equations, for the shear and vorticity tensors:

$$\frac{d\mathbf{E}}{dt} + \mathbf{E}^2 + \mathbf{\Omega}^2 = -\mathbf{P} + \nu \nabla^2 \mathbf{E}$$

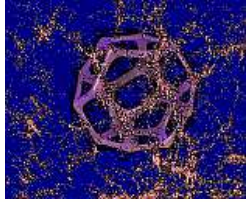
$$\frac{d\mathbf{\Omega}}{dt} + \mathbf{\Omega}\mathbf{E} + \mathbf{E}\mathbf{\Omega} = \nu \nabla^2 \mathbf{\Omega}$$

NB: \mathbf{E} is not divergence-free unless incompressible.

Also, if initially $\mathbf{\Omega} = \mathbf{0}$ then it is always zero.

In the Zel'dovich approximation the right-hand sides are zero.

Density Log density	$\rho, \log \rho$
Gravitational tidal field	$T_{ij} = \frac{\partial^2 \phi}{\partial x_i \partial x_j},$ $\nabla^2 \phi = 4\pi G(\rho - \rho_0)$
Velocity Divergence	$\theta = -\nabla \cdot \mathbf{v} = -\frac{\partial v_k}{\partial x_k}$
Velocity Shear \mathbf{E}	$E_{ij} = \frac{1}{2H_0} \left(\frac{\partial v_i}{\partial x_j} + \frac{\partial v_j}{\partial x_i} \right)$
Rotation tensor $\mathbf{\Omega}$	$\Omega_{ij} = \frac{1}{2H_0} \left(\frac{\partial v_i}{\partial x_j} - \frac{\partial v_j}{\partial x_i} \right)$



Local structural evolution

“Going with the flow”, ie: with a small volume of particles

Consider the matrix $\mathbf{V} : \{\mathbf{V}\}_{ij} = \frac{\partial v_i}{\partial x_j}$

Write eigenvalues as $\lambda_1 \geq \lambda_2 \geq \lambda_3$

These satisfy the characteristic equation of \mathbf{V}

$$\lambda^3 + P\lambda^2 + Q\lambda + R = 0$$

Where

$$P = -\text{tr } \mathbf{V} = -\theta = -(\lambda_1 + \lambda_2 + \lambda_3)$$

$$Q = \frac{1}{2} [P^2 - \text{tr } \mathbf{V}^2] = \frac{1}{2} [P^2 - E^2 - \Omega^2]$$

$$= \lambda_1\lambda_2 + \lambda_2\lambda_3 + \lambda_3\lambda_1$$

$$R = -|\mathbf{V}| = \frac{1}{3} [-P^3 + 3PQ - \text{tr } \mathbf{V}^3]$$

$$= -\lambda_1\lambda_2\lambda_3$$

If the flow is incompressible $P = 0$

The invariants P, Q, R completely characterise the fluid trajectories in general compressible flows.

This provides a classification of the topologically distinct flow patterns and flow singularities in 3D.

This was first done for general 3D fluid flows by

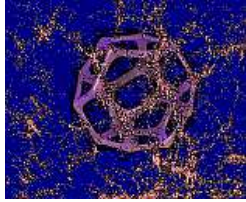
M.S. Chong, et al. 1990, *Physics of Fluids A: Fluid Dynamics*, 2, 765.

“A general classification of three-dimensional flow fields”.

And recently applied to cosmological flows by

X. Wang et al., (arXiv 1309.5305)

“Kinematic Morphology of Large-scale Structure: Evolution from Potential to Rotational Flow “



Vorticity in Collisionless gas

Hahn et al., 2014 arXiv 1404.2280
 “The Properties of Cosmic Velocity Fields”

Vorticity in a collisionless gas:

- Arises in shell-crossing
- Principle axis of shear does not align with vorticity axis
- Halo spin aligned with vorticity on scales $> 4R_{vir}$.
- Large scale structure is dominated by cosmic shear.

*Libeskind 2014:
 Lorentz Workshop talk.*

Vorticity equation in a “classical” fluid:

$$\frac{\partial \boldsymbol{\omega}}{\partial t} + \nabla \times (\boldsymbol{\omega} \times \mathbf{u}) = \frac{1}{\rho^2} \nabla \rho \times \nabla p$$

Baroclinic vorticity generation occurring in shocks. (Binney, 1974; Pichon and Bernardeau, 1999; Hahn et al. 2014)

Ensemble averaged 3-velocity:

$$\langle \mathbf{v} \rangle = \frac{\int_{\mathbf{v}} \mathbf{v} f(\mathbf{x}, \mathbf{v}) d^3 \mathbf{v}}{\int_{\mathbf{v}} f(\mathbf{x}, \mathbf{v}) d^3 \mathbf{v}}$$

With this is it can be shown that

$$\nabla \cdot \langle \mathbf{v} \rangle = \langle (\mathbf{v} - \langle \mathbf{v} \rangle) \cdot \nabla \log \rho \rangle + \langle \nabla \cdot \mathbf{v} \rangle$$

$$\nabla \times \langle \mathbf{v} \rangle = \langle (\mathbf{v} - \langle \mathbf{v} \rangle) \cdot \nabla \log \rho \rangle + \langle \nabla \times \mathbf{v} \rangle$$

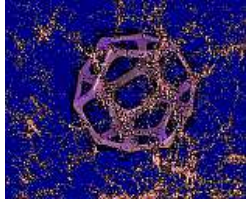
Initial conditions are such that $\langle \nabla \times \mathbf{v} \rangle = \mathbf{0}$

Phase space circulation theorem:

$$\frac{D}{Dt} \int \mathbf{v}(\mathbf{s}) d\mathbf{s} = 0$$

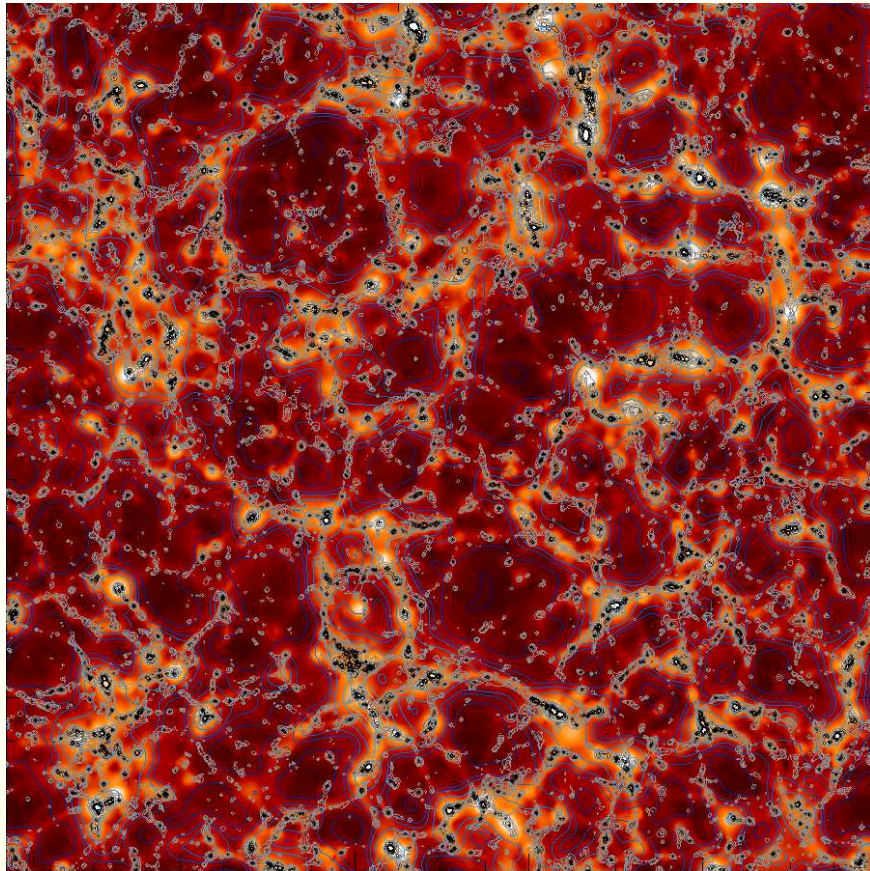
$$\frac{D}{Dt} \equiv \frac{\partial}{\partial t} + \mathbf{v} \cdot \frac{\partial}{\partial \mathbf{r}} + \nabla \phi \cdot \frac{\partial}{\partial \mathbf{v}}$$

(Lynden-bell 1967: *Violent relaxation*)

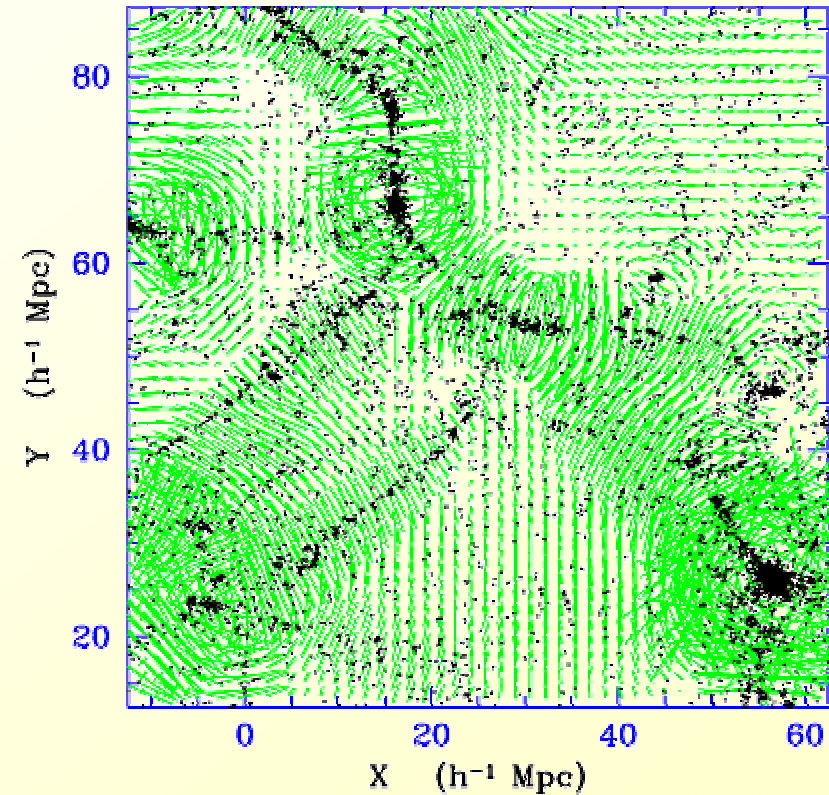


Action of the tidal field

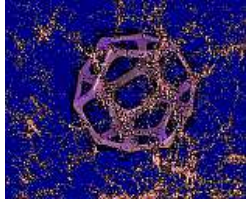
Relationship between density field and the gravitational tidal field



The magnitude of the tidal field is coded in red.
 Blue density contours reflect density smoothed 6 Mpc/h
 Grey contours are particle distribution

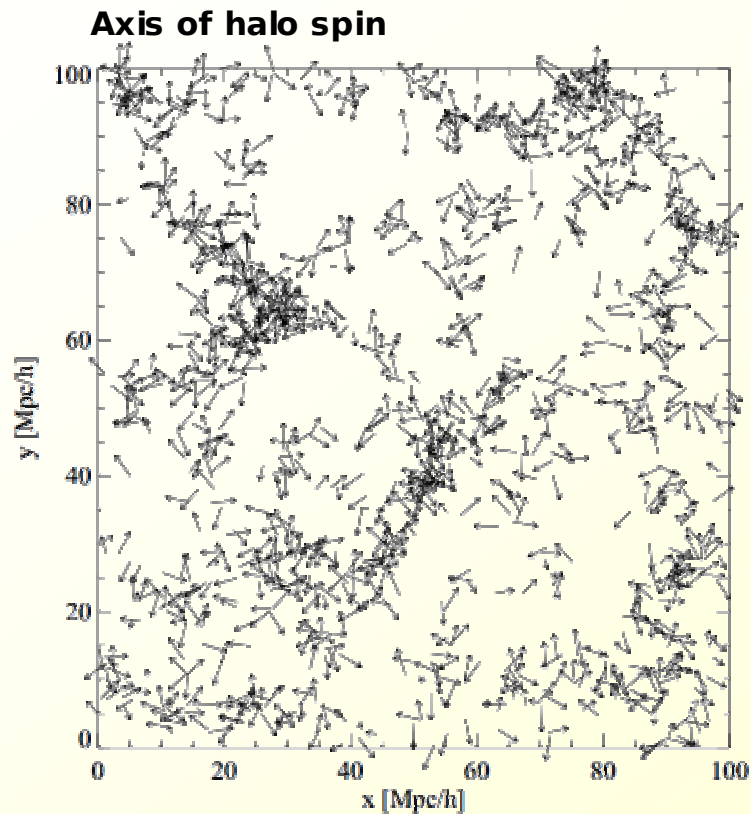


Distribution of DM particles in black.
 The green lines show the size and direction of
 the greatest compression eigen-direction.
 Of course maximal compression in filaments is
 perpendicular to filament direction.

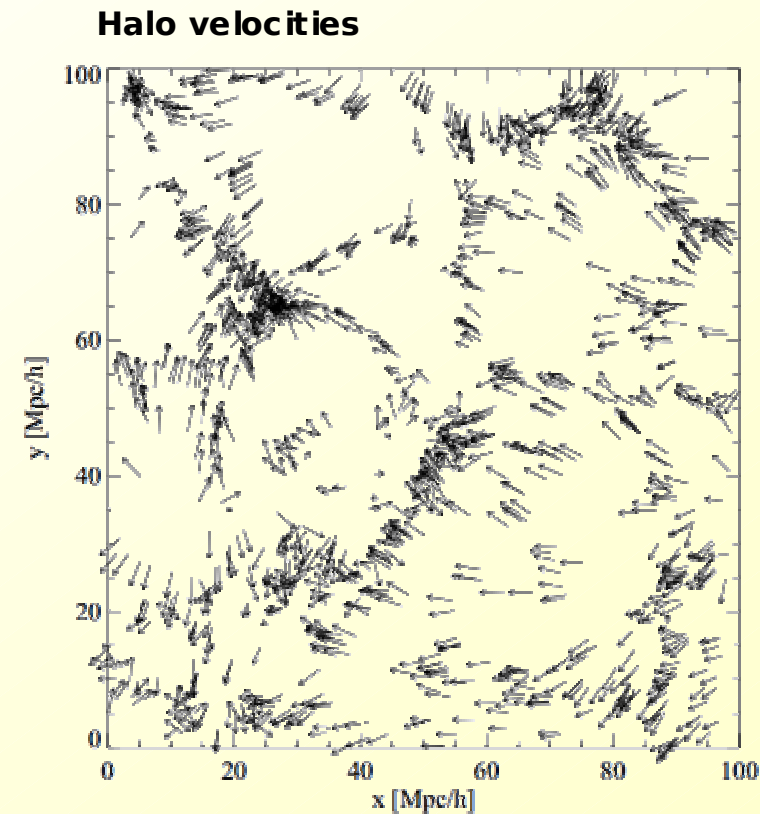


Systemic motion and halo spins

From “*Spinning Galaxies within the Large Scale Structure of the Universe*”
Holly Trowland (Ph.D. Thesis, University of Sydney, 2013).

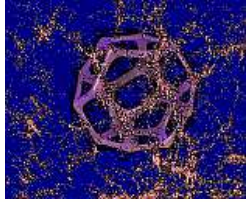


Halo Spin orientations are not manifestly ordered.
Discovering systemic effects requires sophisticated procedures



Filaments have systemic movement and galaxies that comprise the filaments sometimes fall towards the local cluster, but not always.

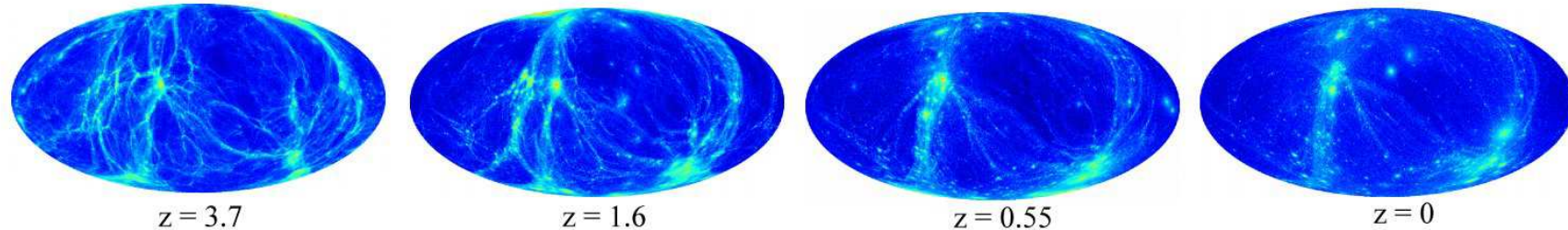
“The Cosmic History of the Spin of Dark Matter Halos within the Large-scale Structure”
H.E. Trowland, G.F. Lewis, J. Bland-Hawthorn, *Astrophysical Journal*, 2013, **762**, 72.



The sky-view of filament motion

Rieder et al. 2013 arXiv 1307.7182

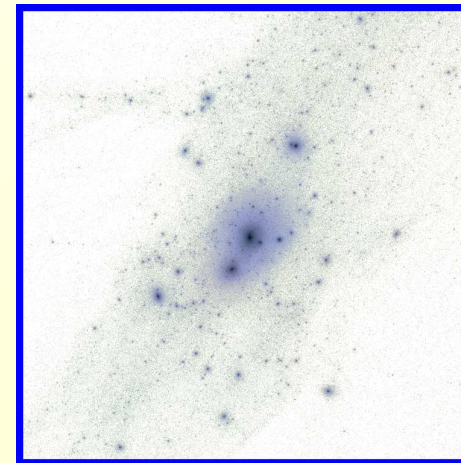
Assembly of filamentary void galaxy configurations



The diagrams show the evolution of a $1h^{-1}$ Mpc radius sphere, as seen from a “void galaxy” at the centre of the sphere.

The void galaxies were selected geometrically from the CosmoGrid high resolution N-Body simulation.

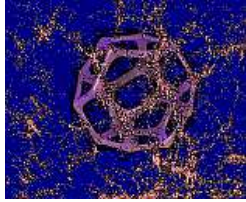
Note the filament dynamics.



CosmoGrid Void system CGV-D

Ishiyama T. et al., 2013, ApJ, 767, 146

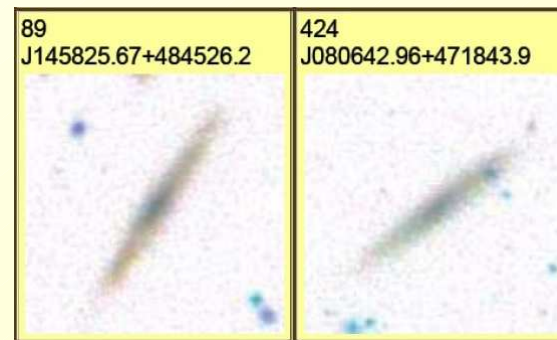
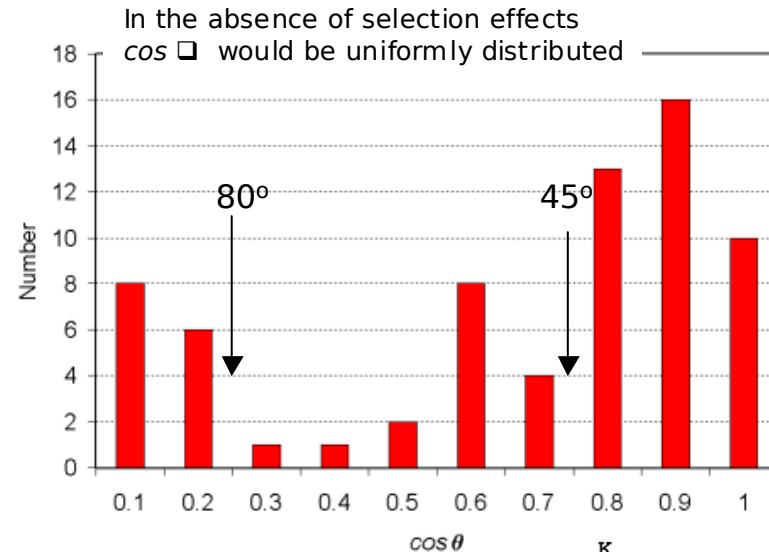
$2048^3 \Lambda$ CDM hi-res simulation in $21h^{-1}$ Mpc box.
Particle mass = $8.9 \times 10^4 M_{\text{SUN}}$



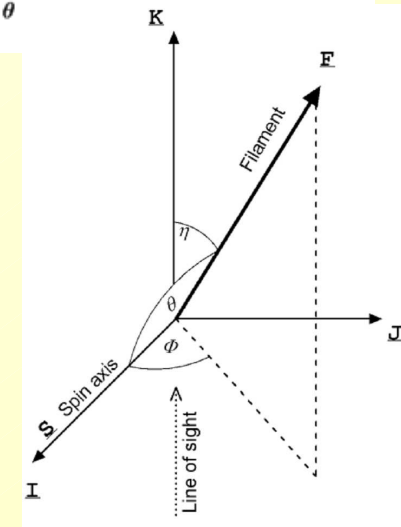
Orientations in MMF Filaments

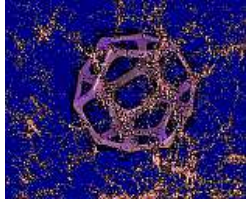
From "Fossil evidence for spin alignment of Sloan Digital Sky Survey galaxies in filaments"
 B.J.T. Jones, R. van de Weygaert, M. Aragon-Calvo (2010) M.N.R.A.S. , **408**, 897-918

- ❑ Sloan DR5 has ~100,000 galaxies having $0.01 < z < 0.11$ within the slice $\eta_{\text{sloan}} < 40^\circ$. Construct an MMF filament catalogue from these.
- ❑ Find all edge-on galaxies ($b/a < 0.2$) in these filaments. This yields 492 galaxies in 426 filaments.
- ❑ Classify the filaments – eyeball them – Class A (excellent), B, C (poor)
 - Not too sparse
 - Not branched structure
 - Clearly defined in all three projections
- ❑ Prune galaxy sample. Galaxy must
 - be on or near filament
 - not lie near end of filament



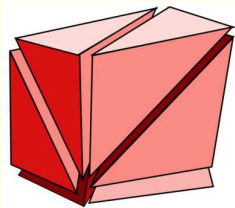
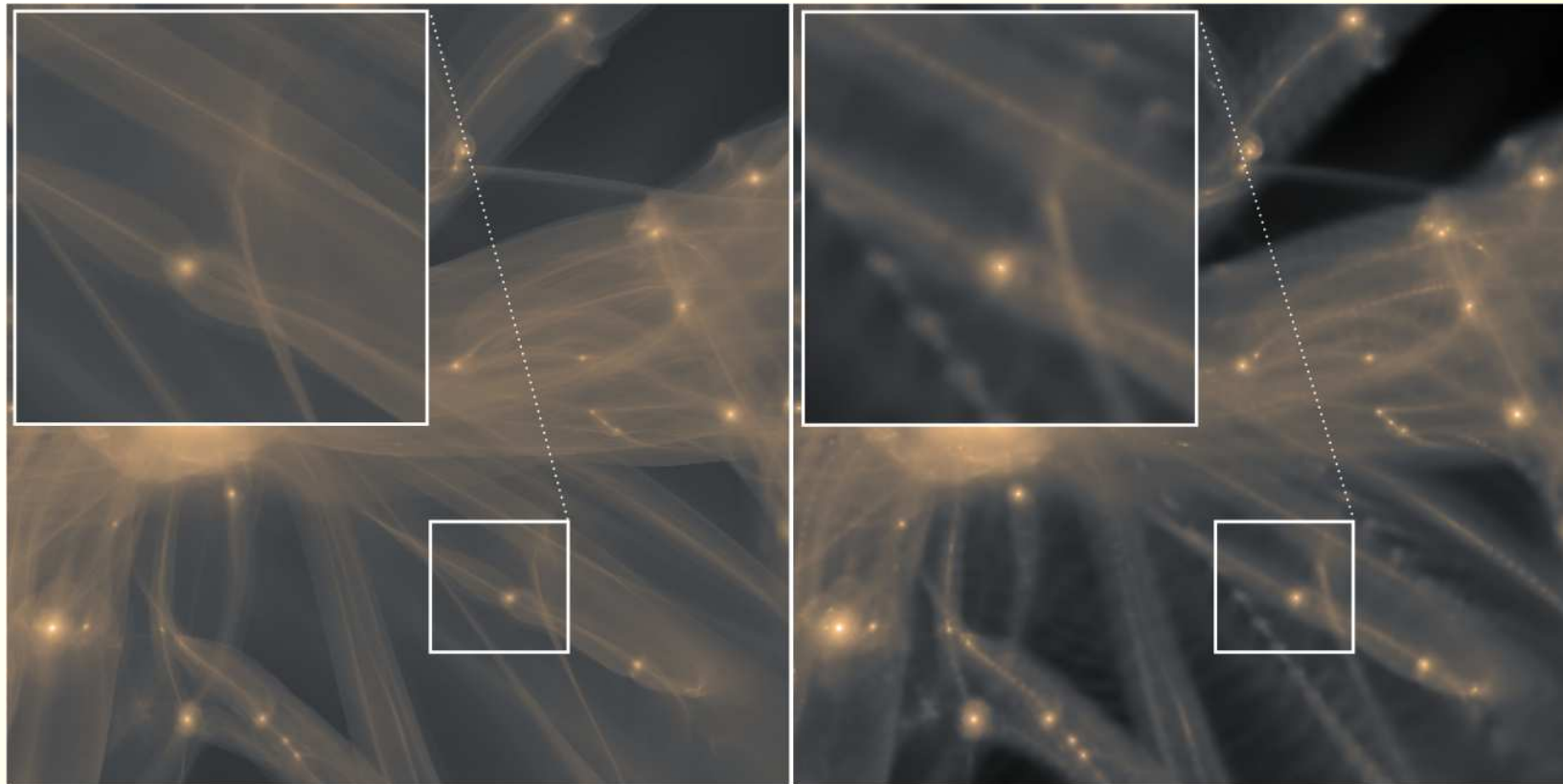
Typical edge-on galaxies in the sample



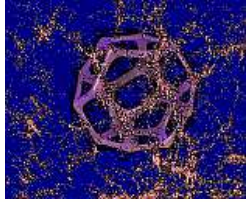


Tetrahedral Rendering

R. Kaehler, O. Hahn, T. Abel. "A Novel Approach to Visualizing Dark Matter Simulations"
IEEE VGTC, Volume 18, Number 12, Dec. 2012 (<http://arxiv.org/abs/1208.3206>)

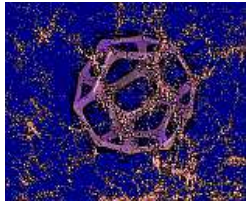


A direct comparison between our tetrahedral cell-projection approach (left) and a standard SPH adaptive kernel smoothing method. Artefacts due to the poor density estimates in low-density regions are obvious for the SPH method, whereas the tetrahedral approach achieves an overall high image quality, on small and large structures. (*Quote from original caption*)



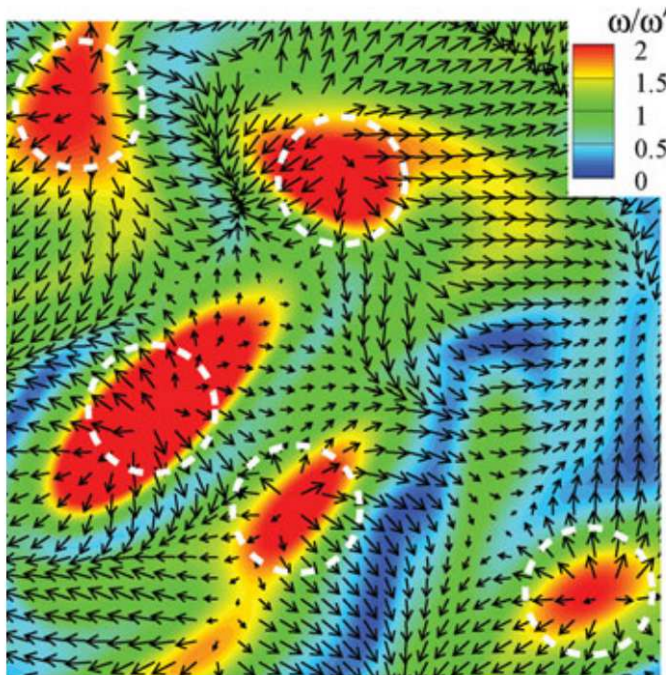
What next?

- At least three fronts:
 - Simulation
 - dynamical modelling
 - observational data
- All of these benefit from better visualisation methods: we are in the world of “big data”.
- But looking at the prettified data and saying “gee whiz” is not enough.

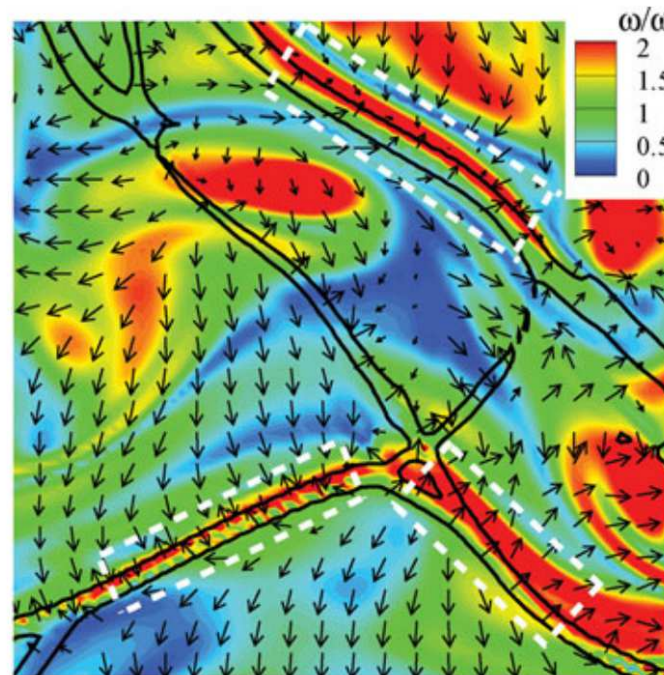


Compressible “turbulence”

Direct numerical simulation of moderate Mach number compressible turbulence.
 J. Wang et al. (2013) *Journal of Turbulence*, **14**, 21-37.



Contours of vorticity magnitude with pressure gradient vectors in smooth regions on a slice.



Contours of vorticity magnitude and dilatation with pressure gradient vectors near shock regions on a slice. The black lines are the shocks.

There is a strong correlation between pressure and vorticity near the shocks.
 Vorticity is amplified immediately downstream of the shocks.
 Leads to a parallel alignment between the pressure gradient and vorticity magnitude gradient near shocks.

Mean Mach number ~ 0.73
 High Mach number ~ 2.5
 Reynolds number ~ 210
 Prandtl number ~ 0.7

Turbulence forced on large scales \rightarrow large scale shocks.
 Pressure and density power spectra $\propto k^{-2}$.

Grid 1024^3

TH-1A supercomputer at Tianjin, China.
 Integrated using seventh-order WENO scheme in shocked regions.